Multigenerational Proteolytic Inactivation of Restriction Upon Subtle Genomic Hypomethylation

Esther Shmidov[1,2], Alexis Villani[3], Senén D. Mendoza[3], Ellay Avihu[1,2], Ilana Lebenthal-Loinger[1], Sarit Karako-Lampert[1], Sivan Shoshani[1,2], Chang Ye[4], Yiding Wang[5], Hao Yan[4,6], Weixin Tang[4,6], Joseph Bondy-Denomy[*,3], Ehud Banin[*,1,2]

[1]The Mina and Everard Goodman Faculty of Life Sciences faculty, Bar-Ilan University, Israel.

[2]Institute of Nanotechnology and Advanced Materials, Bar-Ilan University, Israel.

[3] Department of Microbiology and Immunology, University of California, San Francisco, USA.

[4]Department of Chemistry, The University of Chicago, Chicago, IL, USA.

[5]Department of Biochemistry and Molecular Biology, The University of Chicago, Chicago, IL, USA.

[6]Institute for Biophysical Dynamics, The University of Chicago, Chicago, IL, USA.

[*] Co-corresponding authors

Abstract

15   Restriction-modification (R-M) systems, present in most bacterial genomes,

16   protect against phage infection by detecting and degrading invading foreign DNA.

17   However, like many prokaryotic anti-phage systems, R-M systems pose a

18   significant risk of auto-immunity, exacerbated by the presence of hundreds to

19   thousands of potential cleavage sites in the bacterial genome. In *Pseudomonas*

20   *aeruginosa*, restriction inactivation upon growth at high temperatures was

21   previously described, however, which system is being inactivated, the underlying

22   mechanism, as well as the timing of recovery, remain unknown. Here, we report

23   that *P. aeruginosa* Type I methyltransferase (HsdMS) and restriction

24   endonuclease (HsdR) components are degraded by two Lon-like proteases when

25   replicating above 41 °C, which induces partial genome hypomethylation and

26   simultaneously prevents self-targeting, respectively. Interestingly, upon return to

27   37 ºC, methyltransferase activity returns gradually, with restriction activity not fully

28   recovering for over 60 bacterial generations, representing the longest bacterial

29   memory to our knowledge. Forced expression of HsdR over the first 45

30   generations is toxic, demonstrating the fitness benefit of HsdR inactivation. Our

31   findings demonstrate that type I R-M is tightly regulated post-translationally with a

32   remarkable memory effect to ensure genomic stability and emphasize the

33   importance of mitigating auto-toxicity for bacterial defense systems.

Introduction

34

35 Bacteriophages (phages) are viruses that infect bacteria. Over millions of years
36 of co-evolution, bacterial strains have evolved various anti-phage defense
37 systems[1]. The first discovered genes to have anti-phage activity were the
38 Restriction-Modification (R-M) systems[2]. However, despite their early discovery,
39 many fundamental aspects of R-M system biology remain poorly understood. To
40 date, over 100 additional defense systems have been identified[3], varying in the
41 mechanism of action, phage targets, and viral sensing[4]. Alongside their
42 protective role, bacterial defense systems often feature nucleases or other
43 potentially toxic enzymes, generating a risk for autoimmunity[5] and need to be
44 tightly regulated to become activated only for defense purposes.

45 R-M systems protect the bacterial cell from phage infection by detecting and
46 degrading invading foreign DNA. Most bacterial genomes (83%) carry at least
47 one R-M system[6]. These systems modify the bacterial genome at system-specific
48 modification sites with the methyltransferase component and subsequently
49 degrade the viral genome with the restriction endonuclease holoenzyme upon
50 detection of unmodified sites in the invading DNA. In terms of autoimmunity and
51 toxicity, R-M systems hold a great risk as the restriction motifs are located within
52 the bacterial chromosome in high numbers. One example of autoimmunity
53 avoidance from type I R-M systems in *Escherichia coli* is restriction alleviation
54 (RA), where the protease ClpXP degraded the endonuclease to prevent self-
55 targeting after DNA damage[7,8,9]. For *Pseudomonas aeruginosa*, an opportunistic
56 gram-negative pathogen[10], type I R-M represents one of the most abundant
57 defense systems among the isolates[11]. In the PAO1 laboratory strain, a
58 commonly used laboratory strain of P. aeruginosa, an active type I R-M system is
59 encoded by the three proximal genes PA2735 (*hsdM)*, PA2734 (*hsdS*), and
60 PA2732 (*hsdR*) with a modification pattern of the GATC(N)$_6$GTC sequence[12,13].
61 HsdMS form the active methyltransferase while the HsdMSR holoenzyme is the
62 endonuclease[14] (Fig. 1A).

63 In 1965, Holloway reported the inactivation of restriction activity when *P.*
64 *aeruginosa* was grown at 43 ⁰C[15]. However, which R-M system was being
65 controlled in this experiment, and the mechanism of action are not understood.
66 Here, we show that the Type I R-M is inactivated in *P. aeruginosa* upon multiple
67 rounds of cell division and nascent DNA synthesis at elevated temperatures (>41
68 ⁰C), which induces genomic hypomethylation. Notably, transient heat shock, DNA
69 damage, or prolonged exposure to high temperatures during the stationary phase
70 do not induce restriction inactivation. By studying the effects of culturing *P.*
71 *aeruginosa* at elevated temperatures as a model for the consequences of
72 hypomethylation, we demonstrate that methylation deficiency is indeed
73 necessary to induce restriction loss and that Lon proteases are responsible for a
74 partial decrease in the levels of the methyltransferase HsdMS and a strong
75 inactivation of HsdR. Upon return to lower temperatures (i.e. 37 ⁰C), restriction
76 remarkably remains inactive for up to 60 generations and, for most of this period,
77 forced expression of HsdR is toxic. We named this phenomenon iREN for
78 **i**nactivation of **R**estriction **En**donuclease.

Results

Bacterial replication at 43 °C leads to complete inhibition of the type I R-M system

82 We have previously shown that the Type I R-M system in strain PAO1 is active
83 against phage JBD30[13]. Therefore, we first set out to establish that the previously
84 observed loss of restriction activity in 1965[15] in a strain described as "PAO" could
85 be recapitulated and connected to this specific system. To establish this
86 connection, we used JBD30 (containing 5 restriction sites), a related temperate
87 phage JBD24 (6 sites), and the distinct lytic phage Luz24 (5 sites). Modified
88 phages (M) were propagated in the WT PAO1 strain, while unmodified phages
89 (UM) were generated by propagating them in strain PA14, which lacks any Type I
90 R-M system. When UM phages were used to infect WT PAO1 (grown at 37 ⁰C),
91 their efficiencies of plating (EOP) were reduced by approximately 5 orders of
92 magnitude, compared to a Δ*hsdR* strain, indicating successful restriction (Fig.

93   1B). To examine the inactivation of restriction activity, we grew overnight (ON) the
94   PAO1 WT strain, at 43 °C instead of 37 °C. Cells grown at 43 °C showed
95   complete inactivation of restriction endonuclease (which we refer to as the iREN
96   state), phenocopying the Δ*hsdR* mutant. These results demonstrate that the Type
97   I R-M system in PAO1 is inactivated during growth at high temperature.

98   We next investigated the requirements for the establishment of iREN. By
99   culturing WT PAO1 at a range of temperatures, we found partial inactivation at
100   temperatures higher than 40.5 °C and full inactivation at temperatures above 42
101   °C (Fig. S1A). Additionally, we determined the duration required for complete
102   iREN to occur at 43 °C to be a minimum of 3 hours of cell division during the
103   early log phase (Fig. 1C). iREN does not occur with transient heat exposure or
104   long-term exposure during the stationary phase (Fig. S1B). This suggests that
105   cell division and *de novo* DNA synthesis are essential for iREN.

106   Recombination processes, both RecA-dependent and independent, are typically
107   activated in response to DNA damage[16]. To determine if the iREN phenotype
108   depends on these processes, we created mutants in the *rec* genes. Deletion of
109   *recA*, *recB*, and *recC* had no impact on the iREN phenotype (Fig. S2A).
110   Additionally, exposure to UV light or agents causing double-strand DNA breaks,
111   such as fluoroquinolones, did not trigger complete iREN (Fig. S2B). These
112   findings suggest that the iREN phenotype is not dependent on recombination or
113   the SOS response, which was previously implicated in *E. coli* restriction
114   alleviation (RA)[9]. This, along with the clear need for cell division during high-
115   temperature exposure (compared to a transient heat shock), demonstrates that
116   iREN is distinct from RA.

117   **iREN phenotype heritability**
118   To assess the duration of iREN, we passaged PAO1 cultured at 43 °C for multiple
119   generations at 37 °C while quantifying EOP and plating for colony-forming units
120   (CFUs) to track cell doublings. Restriction activity in the population did not fully
121   recover until around 60 generations of cell division, with partial recovery
122   detectable after the first ~25 generations (Fig. 2A). Interestingly, after

123   approximately 60 generations of restriction recovery, iREN can occur again by
124   culturing the bacteria at 43 °C (Fig. S2C). This indicates that iREN is not due to a
125   permanent genetic change.

126   To determine whether an inability to inactivate restriction would lead to cell
127   toxicity, we over-expressed HsdR. Interestingly, HsdR over-expression was
128   highly toxic, but only in cells previously grown at 43 °C (Fig. 2B). Conversely,
129   cells grown at 37 °C could tolerate higher levels of HsdR as could PAO1 $\Delta hsdM$
130   previously grown at 43 °C (Fig. S4). This demonstrates that inactivation of HsdR
131   is required for cell fitness after growth at 43 °C and that the observed HsdR-
132   induced toxicity is likely due to nucleolytic activity by HsdMSR on unmethylated
133   sites in the bacterial chromosome.

134   To examine whether restriction activity can be restored sooner than 60
135   generations, we created a tightly controlled HsdR expression strain in the
136   background of $\Delta hsdR$ with no promoter leakiness, verified by assessing
137   restriction activity at 37 °C (Fig. S4). We induced HsdR expression at different
138   time points during recovery of restriction. The results showed that inducible re-
139   activation of restriction remains toxic for over ~45 generations of growth at 37 °C
140   (Fig. 2C). These results demonstrate that bacteria exhibit a memory-like ability to
141   keep HsdR off for multiple generations after growth at 43 °C, which is essential
142   for bacterial fitness. This inactivation of HsdR, however, can be bypassed by
143   HsdR over-expression.

144   The motifs that Type I R-M homologs target vary based on sequence divergence
145   in the HsdS proteins[17]. To determine whether the iREN phenotype is conserved
146   in different strains of *P. aeruginosa*, we tested the *P. aeruginosa* strain PAK,
147   which restricts JBD24 phages produced by either PAO1 or PA14. We found that
148   PAK also exhibits heritable iREN (Fig. 2A). We further infected distinct clinical
149   and environmental strains of *P. aeruginosa* with UM phage JBD30 and
150   demonstrated that although the restriction systems are highly diverse, these
151   strains also become more phage sensitive following growth at 43 °C[18] (Table S1).

Impaired modification activity during 43 °C growth

Since toxicity caused by the forced restriction re-activation indicated HsdMS-dependent self-targeting, we hypothesize that unmodified sites are generated in the bacterial chromosome during 43 °C growth. We first examined the stability of the methyltransferase proteins at elevated temperature conditions by immunoblotting for HsdM and HsdS via epitope tags fused to each protein in separate strains at the native genomic locus. The results clearly show that both HsdM and HsdS are highly unstable during 43 °C growth, as the protein levels were reduced compared to the levels observed at 37 °C (Fig. 3A).

Next, to validate that the decreased protein stability results in methylation deficiency, we directly examined the influence of 43 °C growth on the bacterial chromosome methylation state. For that, we used single-molecule-real-time sequencing (SMRT seq) to analyze the bacterial methylome. Surprisingly, the SMRT seq analysis revealed that while hypomethylation indeed emerges after 43 °C growth, only approximately 8% of the modification sites appeared to be unmodified in the population (Fig. 3B), with 11 shared sites between biological replicates, indicating possible hotspots for deficient methylation.

Given the subtle methylation loss and the complexity of the population, we employed an orthogonal method with higher sensitivity and quantitative abilities, eTAM-seq, to more accurately measure genomic methylation. This method deploys enzymatic modification of genomic DNA to distinguish modified adenines from unmodified adenines via Illumina sequencing[19]. This method similarly revealed a 3% decline in the general methylation of the bacterial genome after 43 °C growth (Fig. 3C). Moreover, decreased methylation percentage is also observed in the recovered population after 10 cell doublings at 37 °C. Remarkably, despite the eTAM-seq and SMRT-seq experiments being executed in independent laboratories and sequenced with distinct methodologies, 10 out of the 11 hypomethylated sites were shared between the two approaches. While it is currently unclear what is unique about these sites that makes them prone to becoming hypomethylated, these data together demonstrate that a surprisingly

182 subtle decrease in genomic methylation explains why HsdR must be turned off
183 and why its forced expression is toxic in an HsdM-dependent manner.

184 To examine whether loss of methylation activity at 43 °C is necessary to induce
185 loss of HsdR activity, HsdMS were over-expressed during growth at 43 °C.
186 Expression of these proteins during the overnight growth at 43 °C was indeed
187 sufficient to restore genomic methylation and abolish iREN (Fig. 3D), confirming
188 that iREN is driven by methylation deficiency. This was further verified by eTAM-
189 seq results, which showed that genomic methylation remained intact when
190 HsdMS was over-expressed (Fig. 3C) Taken together we propose that cell
191 division at 43 °C destabilizes HsdMS, reduces functional methyltransferase
192 levels, leading to incomplete methylation of de novo produced host DNA, which
193 in turn drives the need for iREN. This genomic hypomethylation then recovers
194 slowly over multiple generations, while HsdR must remain inactive.

195 **Post-translational decrease in HsdR protein levels during iREN**
196 In PAO1, *hsdM* and *hsdS* are adjacent genes and presumably co-transcribed,
197 while *hsdR* is located within an adjacent operon, suggesting the possibility of
198 independent transcriptional or translational regulation. To gain a better
199 understanding of the different *hsd* components regulation and to find related
200 factors, we performed both transcriptomics and proteomics analyses following
201 five generations after 43 °C growth and at the end of the restriction recovery
202 period (Fig. S6A and 4A). This specific time point was chosen because it aligns
203 with the observed iREN phenotype, allowing us to focus on the effects of the
204 restriction while minimizing effects from high temperature growth. The results
205 showed that at the transcript level, all three genes showed no significant change
206 comparing cells grown only at 37 °C to those five generations after 43 °C growth
207 (Fig. S6A). At the protein level, we also observed that HsdM and HsdS were not
208 decreased five generations after 43 °C growth. However, according to proteomics
209 measurements, HsdR protein levels were significantly reduced after 43 °C growth
210 and eventually returned to basal levels by the end of the recovery phase (Fig.
211 4A). To validate that HsdR is post-translationally regulated, we performed reverse

212 transcriptase quantitative PCR analysis that showed no significant change in the

213 transcript levels of the *hsd* genes (Fig. S6B). We further analyzed both a

214 transcriptional reporter, a strain carrying *mCherry* instead of the *hsdR* ORF, and a

215 translational reporter, a strain with fused *hsdR-mCherry* in the native genomic

216 context (fused to the full-length ORF of *hsdR*). The reporters were analyzed

217 following either 37 °C or 43 °C growth and showed that only the translational

218 reporter exhibited reduced fluorescence after 43 °C growth (Fig. S6C), further

219 corroborating that the HsdR protein is controlled post-translationally.

220 To track HsdR protein levels, we introduced a FLAG-tag (DYKDDDDK) fusion to

221 *hsdR* in its native genomic locus. Western blot analysis shows a reduction in

222 HsdR protein levels both after culturing at 43 °C and after five generations of

223 recovery at 37 °C (Fig. 4B). We additionally immunoblotted a WT PAO1 strain

224 with an HsdR-specific custom antibody which showed a similar reduction in HsdR

225 levels (Fig. S7). For restriction alleviation previously characterized in *E. coli*, it

226 was shown that the DNA translocation activity of the endonuclease is required for

227 proteolytic control[20]. To assess whether this is also the case for iREN, we

228 introduced a mutation in *hsdR* that is defective in ATP hydrolysis and thus cannot

229 perform DNA translocation (HsdR(A493V)). Western blot analysis showed that

230 the ATPase mutant protein levels stayed intact after 43 °C growth (Fig. 4B).

231 These results indicate that either the translocation is essential for protein

232 regulation or that restriction-competent HsdR triggers the loss of HsdR protein.

233 **Lon-like proteases required for iREN**

234 As shown above, the iREN phenotype is conserved among *P. aeruginosa* strains,

235 so we sought to examine the involvement in iREN of known conserved proteases

236 of *P. aeruginosa*. We generated PAO1 complete ORF deletion mutants of the

237 following proteases: ClpX, LasA, ClpA, AsrA, and Lon. We assessed the

238 restriction activity for the protease mutants at 37 °C and following 43 °C growth.

239 In all protease knockouts, iREN was still observed, however both AsrA and Lon

240 knockouts showed only partial inactivation of the restriction activity (Fig. 4C).

241 AsrA is a Lon-like protease, highly similar (40% a.a. sequence identity) to Lon[21].
242 Both are highly conserved and important proteases of *P. aeruginosa*[22,21].
243 Considering the high similarity between the proteases, we assumed that the
244 partial effect is due to functional compensation. Therefore, we created a double
245 mutant strain lacking both the *asrA* and *lon* genes (Δ*2prot*). Indeed, the restriction
246 activity of the Δ*2prot* strain after growth at 43 °C was almost completely intact
247 (Fig 4D), demonstrating the necessity of these two proteases in iREN. Single and
248 double plasmid complementation restored iREN in the Δ*2prot* background (Fig.
249 S8). With the proteases absent, HsdR protein levels were high after incubation at
250 both 37 ºC and 43 ºC (Fig. 4E). Taken together, the results indicate that Lon and
251 AsrA are necessary components regulating the proteolysis of HsdR.

252 **Fitness cost for iREN deficient strain**
253 Forced expression of HsdR was lethal in 43 °C-grown strain due to the presence
254 of unmodified methylation sites in the bacterial chromosome, which led to self-
255 targeting. This raised the question of how the Δ*2prot* strain, lacking both Lon-like
256 proteases, was viable and survived without inactivating restriction. To query
257 whether a more subtle defect emerges when cells cannot proteolyze HsdR, we
258 co-cultured Δ*2prot* cells with Δ*2prot*Δ*hsdR* cells. The competition results showed
259 that the Δ*2prot*Δ*hsdR* outcompeted the Δ*2prot* strain after six hours of growth at
260 43 °C, whereas the Δ*hsdR* strain showed no advantage over WT under 43 °C
261 growth (Fig. 5A and S9). These results suggest that there is indeed a fitness cost
262 to maintaining an intact Type I R-M system when the regulatory proteases are
263 absent. However, despite this detected defect, the Δ*2prot* strain could still grow at
264 43° C. One possible explanation for the relatively minimal fitness cost of retaining
265 the Type I R-M system without regulatory proteases is that the HsdMS
266 methyltransferase complex may also be stabilized in the absence of proteolysis.

267 For a simple assay to query how active modification is in the cell, we assessed
268 the degree of modification of produced phages. Specifically, we examined
269 whether phages produced from cells grown at 43 °C were modified by comparing
270 their titer on WT PAO1 to Δ*hsdR*. Indeed, for the WT background, approximately

271   90% of the phage population produced by cells at 43 °C was unmodified, as
272   evidenced by a ten-fold reduction in EOP when plated on restrictive WT PAO1.
273   This assay effectively detected the modification deficiency in WT cells grown at
274   elevated temperatures. The modification activity assay, based on phage genome
275   modification, confirmed that most phages produced by the Δ*2prot* strain were
276   modified (Fig. 5B). Moreover, HsdMS methyltransferase levels were more stable
277   in the Δ*2prot* strain at 43 °C (Fig. 5C). Together these findings suggest that Lon
278   proteases reduce the stability of both modification proteins and HsdR during
279   high-temperature growth, which explains why the Δ*2prot* strain does not exhibit a
280   severe growth defect: because HsdMS and methyltransferase activities are
281   largely intact.

282   **Proteases specificity in iREN**
283   This work has implicated two Lon proteases in the decrease of three Type I R-M
284   proteins (HsdMSR) during cell division at temperatures >41 °C. This raises the
285   final question as to which of the R-M proteins are targeted by each protease. We
286   therefore assessed protein levels during initial growth at 43 °C compared to 37
287   °C in different protease mutant backgrounds.

288   The results indicate that the effect of the proteases are differentiated. Lon
289   protease mutant resulted mainly in elevated HsdR protein levels following growth
290   at 43 °C, while deletion of AsrA protease resulted in increased HsdM stability
291   during initial growth at 43 °C. Finally, for HsdS, an additive effect was observed
292   as the single protease mutants showed only a slight increase in protein levels,
293   suggesting that both proteases act on HsdS (Fig. 6).

294   These findings suggest a complex regulatory mechanism in which Lon and AsrA
295   proteases collaboratively down-regulate the levels of HsdR, HsdM, and HsdS
296   proteins at 37 °C and 43 °C. These activities are likely required for the genetic
297   maintenance of Type I R-M systems by inactivating the endonuclease
298   holoenzyme when genomic hypomethylation emerges.

299   **Discussion**

300 Holloway first described restriction inactivation at high temperatures, identifying a

301 heritable restriction loss phenotype under such conditions [15]. Our findings

302 identified the inactivated type I R-M system, demonstrated that this is a common

303 property of *P. aeruginosa* isolates, and implicated subtle hypomethylation in the

304 genome as the driver. To this end, we identified that only a minority of genomic

305 methylation sites become unmodified during high-temperature growth. Moreover,

306 we found that both hypomethylation and the iREN phenotype are proteolytically

307 regulated by Lon-like proteases in a collaborative manner (Fig. 7).

308 iREN exhibits a novel type of temporal restriction loss of the type I R-M system

309 when the bacterial genome becomes undermethylated. RA in *E. coli* is induced

310 upon acquiring a new type I R-M system and exposure to UV and other DNA-

311 damaging agents. Recently, it was also shown to be activated through plasmid-

312 carrying hemi-modified recognition sites[9]. Unlike RA, we found that iREN for *P.*

313 *aeruginosa* is not induced upon DNA breaks and is a *recA* and *recBC*-

314 independent process. This suggests that iREN is closely associated with the

315 instability of HsdMS, as stable HsdMS in *P. aeruginosa* sustain normal

316 methylation rates even when recombination processes create hemi-modified

317 sites. The recovery from iREN took up to 60 generations, starting with only 3-8%

318 of unmodified sites in the genome. In contrast, for RA, when acquiring a new

319 system with a fully unmodified chromosome, only a lag of 15 generations was

320 described[7] indicating either a faster modification rate of the *EcoKI* system or,

321 alternatively, a tighter regulatory mechanism for iREN.

322 The observed high sensitivity to complete restriction inhibition, even with only a

323 slight decrease in methylation, highlights the critical need for strict autoimmunity

324 regulation in bacterial defense systems, as nearly all bacterial defense systems

325 possess autotoxicity and must be tightly controlled to prevent unnecessary

326 activation. Systems operating through abortive infection (Abi) mechanisms inhibit

327 cellular metabolism or program bacterial cell dormancy/death upon infection to

328 prevent viral replication. For example, Toxin-Antitoxin (TA)[23] systems neutralize

329 toxins via labile antitoxins until changes in cellular physiology license toxin

330 activity. Direct defense systems, such as R-M and CRISPR-Cas[24] systems, also
331 exhibit autotoxicity from off-target nucleolytic cleavage of host DNA or
332 deficiencies in protective mechanisms. While our findings focused on type I R-M,
333 this temperature-induced restriction loss serves as a valuable model for
334 understanding how genomic methylation may be compromised and responded
335 to. Moreover, based on our results, these mechanisms presumably vary between
336 bacterial species and should be investigated in other hosts.

337 Our findings suggest that Lon proteases have a dual regulatory role: they initially
338 cause hypomethylation during high-temperature growth by reducing modification
339 activity, but also degrade HsdR to limit generation of toxic double-stranded
340 breaks in the bacterial chromosome and provide time for restored methylation.
341 The restriction recovery process itself was found to be highly reproducible but
342 gradual, consistently occurring after a specific number of bacterial cell divisions.
343 This moderated recovery could result from population heterogeneity, where a
344 subset of cells fully recovers and eventually dominates the culture over 60
345 generations, or from chromosomal re-modification, where the proteases degrade
346 the restriction component, leading to partial inhibition and reflecting the
347 chromosomal methylation status. Understanding these mechanisms will require
348 further studies at the single-cell level.

349 These insights have practical implications in laboratory settings. iREN represents
350 a rapid and simple experimental perturbation to bypass a common bacterial
351 defense, which is particularly important when working with phages that infect
352 multiple related strains. Given the observed memory phenotype of iREN,
353 understanding its effects on the host is essential to manage and control its
354 application in laboratory experiments. In conclusion, this study reveals the
355 importance of precise negative regulation of a bacterial defense system to
356 maintain genomic integrity with memory to ensure safety. Our findings highlight
357 how bacteria quickly adapt to methylation deficiencies, using high-temperature
358 growth as a model for understanding these responses.

Author contributions statement

E.S., A.V., S.D.M., and I.A. generated strains and conducted phenotypic experiments and analyses. E.S. drafted the initial manuscript, and A.V., S.S., E.B., and J.B.D. reviewed and edited the text. Y.W. and H.Y. prepared the eTAM-seq libraries, while C.Y. performed the next-generation sequencing and bioinformatics analysis, with additional analysis contributions from I.L.L. W.T. supervised the eTAM-seq work. S.L. contributed to the methodology. E.B. and J.B.D. provided overall supervision and secured funding.

Competing Interests

J.B.D. is a scientific advisory board member of SNIPR Biome, Excision Biotherapeutics, and LeapFrog Bio, consults for BiomX, and is a scientific advisory board member and co-founder of Acrigen Biosciences and ePhective Therapeutics. The Bondy-Denomy lab received research support from Felix Biotechnology. Patent application no. 63/417,245 has been filed for eTAM-seq by the University of Chicago. The authors declare no other competing interests.

389 **Data availability**

390 All strains and plasmids utilized in this study are detailed in Table S2. The raw

391 data from SMRT-seq, RNA-seq, and liquid chromatography-mass spectrometry

392 have been deposited and are available at:

393 https://doi.org/10.25452/figshare.plus.c.7498956.

394 # Materials and Methods

395 **Bacterial strains, plasmids, and phages**

396 The bacterial strains, phages, and plasmids used in this study are detailed in

397 Supplementary Table S2. Unless stated otherwise, all strains were grown in LB

398 (Luria-Bertani broth, Difco) at 37 °C. For deletion mutant creation, the following

399 media were used: Vogel Bonner Minimal Medium (VBMM)[25], Pseudomonas

400 Isolation Agar (PIA, Difco), and No salt Luria-Bertani (NSLB) supplemented with

401 10% sucrose. For DH5α heat shock, BHI (brain heart infusion broth, Difco) media

402 was used. All strains were grown at 37 °C unless otherwise specified. Antibiotic

403 concentrations used in this study were 300 µg/mL Carbenicillin (Crb) and 50

404 µg/ml Gentamicin (Gm) for *P. aeruginosa*, 100 µg/mL Ampicillin (Amp), and 30

405 µg/mL Gm for *Escherichia coli*.

406 **Plasmids construction**

407 The genomic extraction was carried out using the DNeasy Blood& Cell Culture

408 DNA Kit (Qiagen). For DNA fragment amplification, Phusion® High-Fidelity DNA

409 Polymerase (Thermo) was used. For gene overexpression, primers were

410 designed to complement the beginning and end of each gene, with the addition

411 of either enzyme restriction sites for ligation or an overlap sequence for Gibson

412 assembly. The amplified inserts were purified using NucleoSpin® Gel and PCR

413 Clean-up (MACHEREY-NAGEL). For the ligation assay, inserts and plasmids

414 were digested using the appropriate fast-digest restricted enzymes (Thermo).

415 Ligation was conducted using Biogase - fast ligation kit (Bio-Lab Ltd.). For the

416 Gibson assembly, inserts were incubated in the appropriate concentration with a

417 linearized plasmid and 2X LigON mixture (EURX). For plasmid extraction, the

418 QIAprep spin mini-prep kit (QIAGEN) was used. For verification of successful

419   plasmid transformations, the DNA Polymerase ReddyMix™ PCR Kit and

420   universal primers were used.

421   **Efficiency of plaquing (EOP) assay**

422   For phage extraction, overnight cultures of JBD24 lysogenic bacteria were

423   prepared, with PAO1 for modified and PA14 for UM phages. These cultures were

424   diluted 1:50 with fresh medium and incubated until reaching an optical density

425   (OD) of 0.5 at 595 nm. Phage induction was initiated by adding 0.4 µg/ml

426   Norfloxacin (NOR, Sigma) antibiotic, followed by an additional incubation period

427   of 1 hour. Fresh LB medium was then added, constituting 50% of the culture

428   volume, and the cultures were further incubated for an hour to facilitate phage

429   amplification. Subsequently, the bacterial cells were centrifuged at maximum

430   speed, and the supernatant was filtered using a 0.45 µm filter (Whatman).

431   For Efficiency of Plaquing (EOP) calculation, overnight cultures of host bacteria,

432   grown at either 37 °C or 43 °C, were used. Soft-agar LB containing 0.5% agar,

433   preheated to 50 °C, was gently mixed with a volume of 100 µl of the overnight

434   host cultures and poured onto the surface of a solidified agar plate containing

435   1.5% agar. After appropriate air-drying, serial dilutions of the examined phages

436   were plated in drops of 2 µl on top of the host-containing soft agar. The plates

437   were then incubated overnight at 37 °C, allowing plaques to form, which could be

438   subsequently counted for the calculation of plaque-forming units per milliliter

439   (PFU/ml).

440   **Restriction and Modification activity calculation**

441   Restriction activity for the examined strain was calculated by its EOP and the

442   EOP of permissive Δ*hsdR* strain with the following formula:

443   $$\text{Restriction Activity} = \log\left(\frac{\text{EOP}_{\Delta hsdR}}{\text{EOP}_{\text{X}}}\right).$$

444   The calculation of modification activity for the examined phage was determined

445   by comparing its EOP in a restrictive strain to the EOP of a permissive Δ*hsdR*

446   strain, using the following formula:

447 $$\text{Modification Activity} = \log\left(\frac{\text{EOP}_{\text{restrictive}}}{\text{EOP}_{\Delta hsdR}}\right).$$

448 **Growth curve**

449 Overnight cultures of the strains were diluted to 0.005 OD (595 nm) in fresh
450 media and transferred to a 96-well plate, 200µl in each well. Arabinose or
451 Rhamnose was added for gene induction (33.3Mm and 0.2% unless otherwise
452 specified). The plates were incubated for 20 hours at 37 °C or 43 °C with
453 agitation. Optical density measurements at 600 nm were taken every 10 minutes
454 using the Synergy™ 2 Multi-Detection Microplate Reader (BioTek).

455 **Restriction recovery assay**

456 For the analysis of restriction activity recovery, overnight cultures grown at either
457 43 °C or 37 °C were assessed for EOP and plating efficiency. These cultures
458 were then sub-cultured by diluting them 1:1000 and incubating them further at 37
459 °C. EOP and plating efficiency measurements were taken every 12 hours
460 thereafter with repeated sub-culturing passaging of the bacteria. From EOP
461 measurements, restriction activity could be calculated, and from plating efficiency
462 measurements, generations were determined using the following formula:
463 $$\text{Generations} = \log_2\left(\frac{\text{CFU}_{\text{end}}}{\text{CFU}_{\text{start}}}\right).$$

464 **Protein extraction**

465 Overnight cultures grown at 37 °C or 43 °C were diluted 1:100 into fresh LB and
466 grown at the examined temperature to 0.8 OD (595 nm). From each strain, 8 OD
467 (595 nm) of bacteria were harvested, centrifuged at 4,000 RPM for 10 minutes,
468 and the supernatant was discarded. The cell pellet was then resuspended in lysis
469 buffer (comprising 100 mM NaCl, 5% Glycerol, and 50 mM Tris pH 7.5)
470 supplemented with Benzonase® Endonuclease (MILLIPORE), cOmplete™
471 protease inhibitor cocktail (ROCHE), and Lysozyme (Sigma-Aldrich).
472 Subsequently, the samples underwent sonication (3 minutes, with cycles of 5
473 seconds on and 5 seconds off, at 54% amplitude). The sonicated samples were
474 then centrifuged at 14,000 g for 10 minutes, and the upper liquid phase
475 containing the proteins was carefully collected.

Western blot

For Western blot analysis, protein samples were diluted with Sample buffer (comprising 150 mM Tris-HCl pH=6.8, 3% β-Mercaptoethanol, 6% Sodium dodecyl Sulfate, 0.3% Bromophenol blue, 30% Glycerol, and water), followed by incubation at 95 °C for 10 minutes. Subsequently, the samples were centrifuged at 14,000g for 2 minutes. The processed samples were then separated on a 20% Tris-Glycine gel and transferred onto a nitrocellulose membrane. For blocking, the membrane was treated with 5% skim milk in TBS, and incubated overnight at 4 °C. Following blocking, the membrane was incubated for 1 hour with anti-FLAG antibodies (diluted at 1:2,500, Sigma-Aldrich). After three washes with TBST (Tris-buffered saline with Tween), the membrane was then incubated with mouse anti-mouse (HRP) antibodies (diluted at 1:10,000, Merck) for an hour. Subsequently, the membrane underwent an additional three washes with TBST before being developed using an ECL kit (Thermo).

Proteomics analysis

For proteomics sample preparation, the samples were subjected to in-solution tryptic digestion using suspension trapping (S-trap method by Protifi). The resulting peptides were analyzed in Liquid chromatography mass spectrometry (LC-MS), using nanoflow liquid chromatography (nanoAcquity) coupled to high resolution, high mass accuracy mass spectrometry (Q-Exactive HF). Each sample was analyzed on the instrument separately in a random order in discovery mode. Raw data was processed with MaxQuant v1.6.6.0. The data was searched with the Andromeda search engine against the *Pseudomonas aeruginosa* PAO1 database as downloaded from Uniprot, appended with common lab protein contaminants. Search parameters included the following modifications: Fixed modification- cysteine carbamidomethylation. Variable modifications- methionine oxidation. The quantitative comparisons were calculated using Perseus v1.6.0.7. Decoy hits were filtered out, and only proteins that were identified in at least two replicates of at least one experimental group were kept.

Samples collection for proteomics and transcriptomics analysis

Overnight bacterial cultures cultivated at either 37 °C or 43 °C were diluted 1:100 into 15 ml fresh LB medium and cultured until reaching an optical density (OD) of 0.6 at 595nm from each sample, 2 ml was centrifuged and stored at -80°C for future RNA and protein extraction, while the remaining culture was further diluted 1:1000 for overnight growth at 37 °C. This process was repeated daily until the fifth incubation. Finally, RNA extraction was performed simultaneously on samples collected at all specified time points as previously decribed[26].

Transcriptomics analysis

For RNA sequencing, 2 ug of total RNA was used for the RiboMinus™ Bacteria Transcriptome Isolation Kit (Invitrogen). The library was constructed with Kapa Stranded RNA-Seq Kit (KK8421) according to the manufacturer's instructions using 30ng of depleted RNA as starting material. The final quality was evaluated by TapeStation High Sensitivity D1000 Assay (Agilent Technologies, CA, USA). Sequencing was performed based on Qubit values and loaded onto an Illumina MiSeq using the MiSeq V2 (50- cycles) Kit Illumina (CA, USA). Paired-end RNA-seq protocol yielded about 3.4-6.5 million paired-end reads per sample. FastQC (v0.11.2) (https://www.bioinformatics.babraham.ac.uk/projects/fastqc) was used to assess the quality of raw reads. Reads were aligned to *P. aeruginosa* PAO1 strain (assembly GCF_000006765.1) using the bowtie2 aligner software (v2.3.2)[27] with default parameters. GTF annotation file for the PAO1 strain was downloaded from Pseudomonas Genome DB (www.pseudomonas.com). Raw read counts for 5708 gene-level features were determined using HTSeq-count[28] with the intersection-strict mode. Differentially expressed genes were determined with the R Bioconductor package DESeq2[29] (Release 3.14). The p-values were corrected with the Benjamini-Hochberg FDR procedure. Genes with adjusted p-values < 0.05 and |log fold change| > 1 were considered as differentially expressed.

Fluorescence reporter assay

535   Overnight cultures of bacterial strains containing the *mCherry*-fused reporter from

536   37 °C or 43°C were sub-cultured to a final concentration of 0.005 OD (595 nm) in

537   fresh media and transferred to a 96-well plate, with 200µL in each well. Following

538   20 hours of incubation at 37 °C with shaking, optical density at 595 nm, and

539   fluorescence, excited at 580 nm and emitted at 610 nm, were measured using

540   the Synergy™ 2 Multi-Detection Microplate Reader (BioTek).

541   **Competition assay**

542   Overnight cultures of strains containing plasmids with constitutive expression of

543   either GFP or *mCherry* were diluted to create mixed cultures with a final

544   concentration of 0.025 from each strain. Samples were collected at the initial time

545   point and after six hours of incubation at either 37 °C or 43 °C by centrifugation at

546   max speed, and the supernatant was removed. For fixation, the samples were re-

547   suspended in 1 ml of 4% paraformaldehyde (PFA) for 1.5 hours on ice, followed

548   by a wash with PBS. Samples were also stained with Hoechst (Thermo) for

549   general staining by incubating the samples with 50µl of 1µg/ml concentration.

550   Washed samples was then analyzed by BD LSRFortessa™, results were

551   analyzed by FlowJo™.

552   **SMRT seq**

553   Pac Bio subreads were mapped to the reference genome *Pseudomonas*

554   *aeruginosa* PAO1 GCA000006765, ASM676v1, for each sample separately,

555   using the pbmm2 tool from the smrttools 10 toolkit (Pac Bio). 6mA modifications

556   were then inferred with the ipdSummary tools. The control model was used in two

557   separate runs. In the first run, samples from group 43 were used as a reference.

558   In the second run, samples from group 37 °C were used as a reference. Sites

559   with IPD-ratio with p-value < 0.05 were considered to have a new modification in

560   the sample, compared with the reference. Each sample was tested with the

561   reference of the same line, e.g. 1_43_5g was tested against 1_43 or 1_37.

562   2_43_22g was tested against 2_43 or 2_37, and so on.

563   **eTAM seq**

564 Genomic DNA was extracted from cells cultured at 37 ⁰C, 43 ⁰C, or after 10
565 generations of recovery at 37 ⁰C. Cells were 1:1 treated with Lysis Buffer (20mM
566 Tris, 2mM EDTA, 1% SDS, 100μg/mL RNase A, and 100μg/mL Proteinase K) for
567 incubation at 37 ⁰C for 30 minutes, followed by 30 minutes at 55 ⁰C. Following
568 cell lysis, the Zymo Genomic DNA Clean and Concentrator™ kit was used as
569 instructed to extract DNA.

570 For each DNA sample, 100 ng was fragmented using NEBNext® dsDNA
571 Fragmentase (NEB, catalog no. M0348S) at 37 °C for 20 min and then
572 denatured in 0.1 M NaOH at 37 °C for 5 min. The denatured DNA was
573 neutralized by 10% HOAc, purified by the Oligo Clean & Concentrator kit (Zymo),
574 and mixed with 0.001% (w:w) spike-in probes containing one 6mA site and one
575 inosine site (GTG TCT GGT GTT CTG TCG TGT GCT ACT C/iN6Me-dA/T CCG
576 ATC TCG CAT C/ideoxyI/T CAC AGT ATT CGT CGT ATG AGA CAC AAC TAC
577 ATG CTT GTC CGC TCT TGT GTC GGC T).

578 The fragmented and denatured DNA was divided into two halves and designated
579 to eTAM-treated and FTO-treated groups. The FTO-treated group was first
580 denatured at 95 °C for 5 min and demethylated by incubating with 200 pmol of
581 FTO and 1× FTO reaction buffer (2 mM sodium ascorbate (Sigma-Aldrich),
582 65 μM ammonium iron(II) sulfate (Sigma-Aldrich), 0.3 mM α-ketoglutarate
583 (Sigma-Aldrich), 0.1 mg ml^{-1} of bovine serum albumin (NEB) and 50 mM
584 Hepes-KOH, pH 7.0) in reaction volume of 50 ul at 37 °C for 1 h. The
585 demethylated DNA was then purified by the Oligo Clean & Concentrator kit.

586 Both FTO-treated and eTAM-treated groups were denatured in 10% DMSO at
587 95 °C for 5 min and deaminated with 200 pmol of TadA8.20 and 1x
588 deamination buffer (50 mM Tris, 25 mM KCl, 2.5 mM MgCl$_2$, 2 mM DTT and
589 10% (v:v) glycerol, pH 7.5) in reaction volume of 10 ul at 44 °C for 3 h and 44 °C
590 - 55 °C with 3-min incubation per degree. The deaminated DNA was denatured
591 by 0.1 M NaOH at 37 °C for 5 min, neutralized by 10% HOAc, and purified by
592 the Oligo Clean & Concentrator kit. The deamination reaction was then repeated

593 at 44 °C for 1 h and 44 °C - 55 °C with 3-min incubation per degree, followed by

594 a final purification using the Oligo Clean & Concentrator kit.

595 The treated DNA in both groups was then prepared for next-generation

596 sequencing using the xGen™ Methyl-Seq DNA Library Prep Kit (IDT, catalog

597 no. 10009824) following the manufacturer's directions. The resulting library was

598 purified by AMPure XP beads (Beckman Coulter, catalog no. A63882) following

599 the manufacturer's directions and submitted for sequencing. After sequencing,

600 paired-end sequencing reads were preprocessed using Cutadapt to remove

601 adapter sequences and polyC tails with the parameters:

602   "-a AGATCGGAAGAGCACACGTCTGAACTCCAGTCAC -a C{20} -A

603 AGATCGGAAGAGCGTCGTGTAGGGAAAGAG -G G{20}".

604 Clean reads were then aligned to the *P. aeruginosa* PAO1 strain (assembly

605 GCF_000006765.1) using the Hisat2-3n[30] aligner software with default

606 parameters, except for --no-spliced-alignment and --base-change A,G. 6mA sites

607 were detected using the hisat-3n-table command, and the 6mA ratio was

608 calculated as the number of unconverted reads over the total coverage at each A

609 site. Putative 6mA sites were selected based on a negative binomial distribution,

610 adapted from previous methods[31], and filtered by a sequencing coverage

611 threshold of 20. For systematic comparisons across multiple conditions, all 6mA

612 sites within GATC(N)$_6$GTC motifs were extracted for analysis.

613 **References**

614 1. Doron, S. *et al.* Systematic discovery of antiphage defense systems in the
615   microbial pangenome. *Science (1979)* **359**, (2018).

616 2. Luria, S. E. & Human, M. L. A nonhereditary, host-induced variation of
617   bacterial viruses. *J Bacteriol* **64**, 557–569 (1952).

618 3. Millman, A. *et al.* An expanded arsenal of immune systems that protect
619   bacteria from phages. *Cell Host Microbe* **30**, 1556-1569.e5 (2022).

620 4. Georjon, H. & Bernheim, A. The highly diverse antiphage defence systems
621   of bacteria. *Nature Reviews Microbiology* vol. 21 686–700 Preprint at
622   https://doi.org/10.1038/s41579-023-00934-x (2023).

623 5. Rocha, E. P. C. & Bikard, D. Microbial defenses against mobile genetic
624   elements and viruses: Who defends whom from what? *PLoS Biol* **20**,
625   (2022).

626 6. Tesson, F. *et al.* Systematic and quantitative view of the antiviral arsenal of
627   prokaryotes. *Nat Commun* **13**, (2022).

628 7. Makovets, S., Doronina, V. A. & Murray, N. E. Regulation of endonuclease
629   activity by proteolysis prevents breakage of unmodified bacterial
630   chromosomes by type I restriction enzymes. *Proc Natl Acad Sci U S A* **96**,
631   9757 (1999).

632 8. Rabinkova, E. V., Torosyan, M. V. & Fradkin, G. E. Restriction alleviation of
633   phage λ in *Escherichia coli* K-12 cells after γ-irradiation. *Radiobiologiya* **27**,
634   563–564 (1987).

635 9. Skutel, M. *et al.* RecA-dependent or independent recombination of plasmid
636   DNA generates a conflict with the host EcoKI immunity by launching
637   restriction alleviation. *Nucleic Acids Res* **1**, 13–14 (2013).

638 10. Pirnay, J. P. *et al. Pseudomonas aeruginosa* population structure revisited.
639   *PLoS One* **4**, (2009).

640 11. Johnson, M. C. *et al.* Core defense hotspots within *Pseudomonas
641   aeruginosa* are a consistent and rich source of anti-phage defense
642   systems. *Nucleic Acids Res* **51**, 4995–5005 (2023).

643 12. Doberenz, S. *et al.* Identification of a *Pseudomonas aeruginosa* PAO1 DNA
644   methyltransferase, its targets, and physiological roles. *mBio* **8**, (2017).

645 13. Mendoza, S. D. *et al.* A bacteriophage nucleus-like compartment shields
646   DNA from CRISPR nucleases. *Nature* **577**, 244–248 (2020).

647 14. Roberts, R. J. *et al.* A nomenclature for restriction enzymes, DNA
648   methyltransferases, homing endonucleases and their genes. *Nucleic Acids
649   Res* **31**, 1805–1812 (2003).

650 15. Holloway, B. W. Variations in Restriction and Modification of Bacteriophage
651   Following Increase of Growth Temperature of *Pseudomonas aeruginosa*.
652   *Virology* **26**, 634–642 (1965).

653 16. IvančicIvančic, I. *et al.* RecFOR Function Is Required for DNA Repair and
654   Recombination in a RecA Loading-Deficient RecB Mutant *of Escherichia
655   Coli.* https://academic.oup.com/genetics/article/163/2/485/6052619.

656   17.   Murray, N. E. Type I Restriction Systems: Sophisticated Molecular
657   Machines (a Legacy of Bertani and Weigle). *MICROBIOLOGY AND*
658   *MOLECULAR BIOLOGY REVIEWS* vol. 64 (2000).

659   18.   Bondy-Denomy, J. *et al.* Prophages mediate defense against phage
660   infection through diverse mechanisms. *ISME Journal* **10**, 2854–2866
661   (2016).

662   19.   Xiao, Y. L. *et al.* Transcriptome-wide profiling and quantification of N6-
663   methyladenosine by enzyme-assisted adenosine deamination. *Nature*
664   *Biotechnology 2023 41:7* **41**, 993–1003 (2023).

665   20.   Makovets, S., Doronina, V. A. & Murray, N. E. Regulation of endonuclease
666   activity by proteolysis prevents breakage of unmodified bacterial
667   chromosomes by type I restriction enzymes. *Proc Natl Acad Sci U S A* **96**,
668   9757–9762 (1999).

669   21.   Kindrachuk, K. N., Fernández, L., Bains, M. & Hancock, R. E. W.
670   Involvement of an ATP-Dependent Protease, PA0779/AsrA, in Inducing
671   Heat Shock in Response to Tobramycin in *Pseudomonas aeruginosa*.
672   *Antimicrob Agents Chemother* **55**, 1874 (2011).

673   22.   Breidenstein, E. B. M., Bains, M. & Hancock, R. E. W. Involvement of the
674   Lon Protease in the SOS Response Triggered by Ciprofloxacin in
675   *Pseudomonas aeruginosa* PAO1. *Antimicrob Agents Chemother* **56**, 2879
676   (2012).

677   23.   Leroux, M. & Laub, M. T. Toxin-Antitoxin Systems as Phage Defense
678   Elements. (2022) doi:10.1146/annurev-micro-020722.

679   24.   Rostain, W. *et al.* Cas9 off-target binding to the promoter of bacterial genes
680   leads to silencing and toxicity. *Nucleic Acids Res* **51**, 3485–3496 (2023).

681   25.   Hmelo, L. R. *et al.* Precision-engineering the *Pseudomonas aeruginosa*
682   genome with two-step allelic exchange. *Nat Protoc* (2015).

683   26.   Shmidov, E. *et al.* PrrT/A, a *Pseudomonas aeruginosa* Bacterial Encoded
684   Toxin-Antitoxin System Involved in Prophage Regulation and Biofilm
685   Formation. *Microbiol Spectr* **10**, (2022).

686   27.   Langmead, B. & Salzberg, S. L. Fast gapped-read alignment with Bowtie 2.
687   *Nature Methods 2012 9:4* **9**, 357–359 (2012).

688   28.   Anders, S., Pyl, P. T. & Huber, W. HTSeq—a Python framework to work
689   with high-throughput sequencing data. *Bioinformatics* **31**, 166–169 (2015).

690   29.   Love, M. I., Huber, W. & Anders, S. Moderated estimation of fold change
691   and dispersion for RNA-seq data with DESeq2. *Genome Biol* **15**, 1–21
692   (2014).

693   30.   Zhang, Y., Park, C., Bennett, C., Thornton, M. & Kim, D. Rapid and
694   accurate alignment of nucleotide conversion sequencing reads with HISAT-
695   3N. *Genome Res* **31**, 1290–1295 (2021).

696   31.   Dai, Q. *et al.* Ultrafast bisulfite sequencing detection of 5-methylcytosine in
697   DNA and RNA. *Nat Biotechnol* (2024) doi:10.1038/s41587-023-02034-w.

698   32.   Wozniak, D. J. & Ohman, D. E. *Pseudomonas aeruginosa* AlgB, a two-
699   component response regulator of the NtrC family, is required for algD
700   transcription. *J Bacteriol* (1991).

701   33.   Simon, R., Priefer, U. & Puhler, A. A broad host range mobilization system
702   for in vivo genetic engineering: transposon mutagenesis in gram negative
703   bacteria. *Nat Biotechnol* 784–791 (1983).

704   34.   Schweizer, H. P. *Escherichia-Pseudomonas* shuttle vectors derived from
705   pUC18/19. *Gene* **97**, 109–112 (1991).

706   35.   Laura R. Hmelo, B. R. et al K. Precision-engineering the *Pseudomonas
707   aeruginosa* genome with two-step allelic exchange. *Nature Rev Drug
708   Discovery* **5**, 1–8 (2016).

709   36.   Choi, K. H. & Schweizer, H. P. mini-Tn7 insertion in bacteria with single
710   attTn7 sites: Example *Pseudomonas aeruginosa. Nat Protoc* (2006).

711   37.   Newman, J. R. & Fuqua, C. Broad-host-range expression vectors that carry
712   the L-arabinose-inducible *Escherichia coli* araBAD promoter and the araC
713   regulator. *Gene* **227**, 197–203 (1999).

714   38.   Doberenz, S. *et al.* Identification of a *Pseudomonas aeruginosa* PAO1 DNA
715   methyltransferase, its targets, and physiological roles. *mBio* **8**, (2017).

716   39.   Wagemans, J. *et al.* Antibacterial phage ORFans of *Pseudomonas
717   aeruginosa* phage LUZ24 reveal a novel MvaT inhibiting protein. *Front
718   Microbiol* **6**, (2015).

719

720
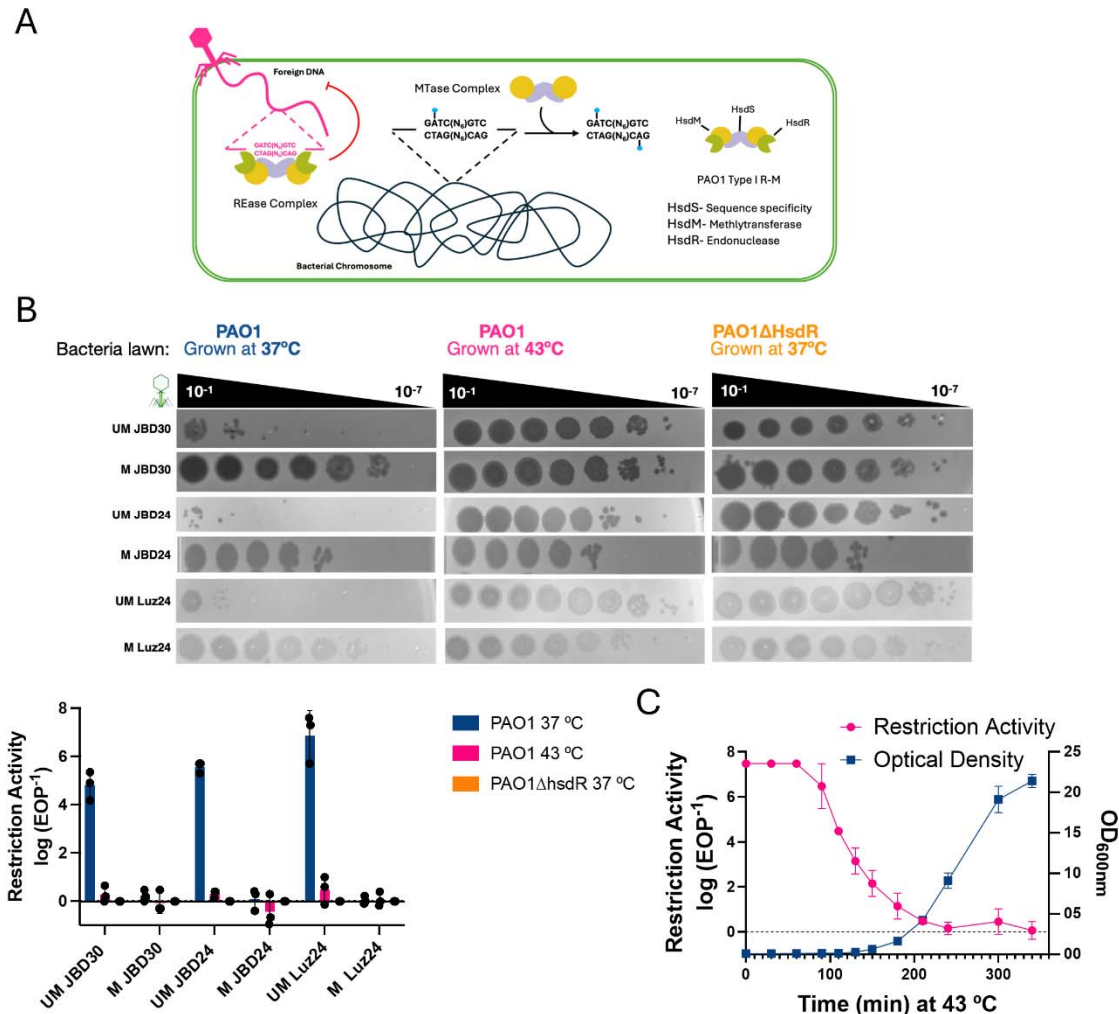
Figure 1: Elevated growth temperature leads to inactivation of restriction endonuclease.
(A) Schematic representation of Type I R-M system. **(B)** Comparative plaquing efficiency and restriction activity of WT grown overnight at either 37 °C or 43 °C and restriction mutant ($\Delta hsdR$) at 37 °C infected with either UM or M phages. **(C)** Log-phase and replication are required for iREN: Restriction activity was examined for PAO1 WT strain during growth at 43 °C at intervals parallel to growth curve measurements through optical density (OD 600nm). The graphs in (B) and (C) represent the average of three independent biological replicates, with error bars indicating standard deviation.

729
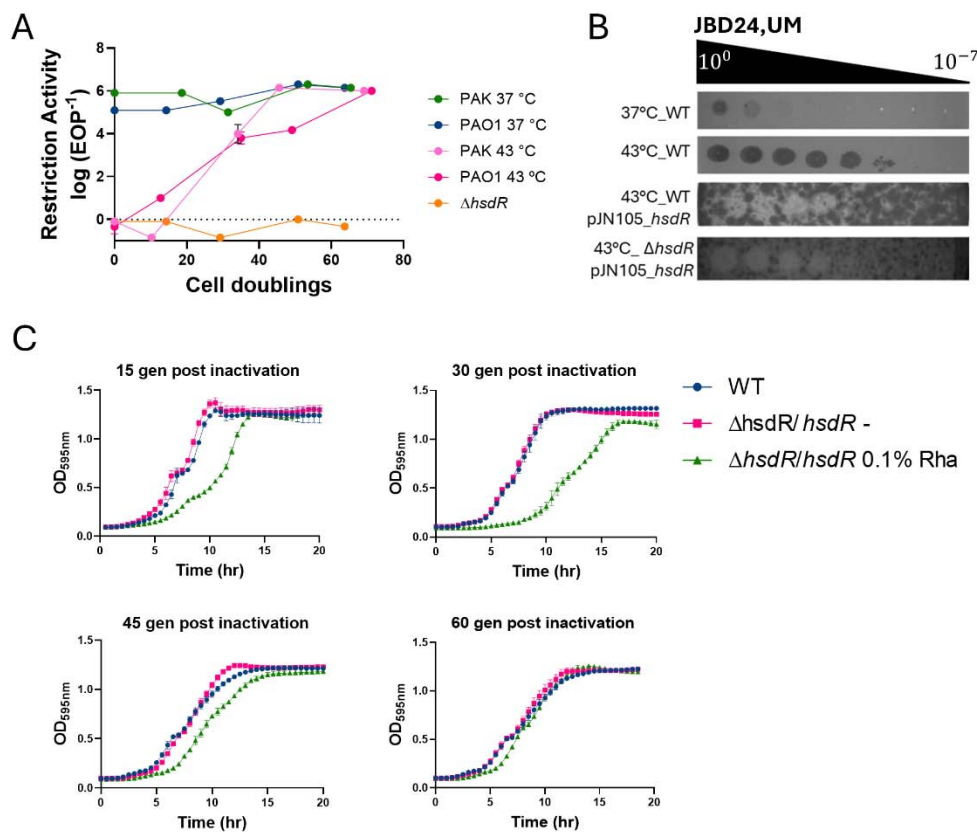
Figure 2: IREN phenotype is heritable and lasts for multiple generations. (A) Recovery of restriction activity over generations at 37°C following overnight growth of WT PAO1 and PAK strains at either 43 °C or 37 °C with Δ*hsdR* as a control. **(B)** Plaquing efficiency comparison of strains with or without *hsdR* OE grown at either 37 °C or 43 °C, including WT and *hsdM* mutant strains, when infected with UM phages. **(C)** Restriction forced activation following 43 °C: Growth curve at 37 °C after ON growth at 43 °C of WT (blue) and strains harboring an inducible copy of *hsdR*, with (green) or without (pink) inducer. The inducer was added at t=0. Generations were counted for the WT strain. The graphs in (A) and (C) represent the average of three independent biological replicates, with error bars indicating standard deviation.

739
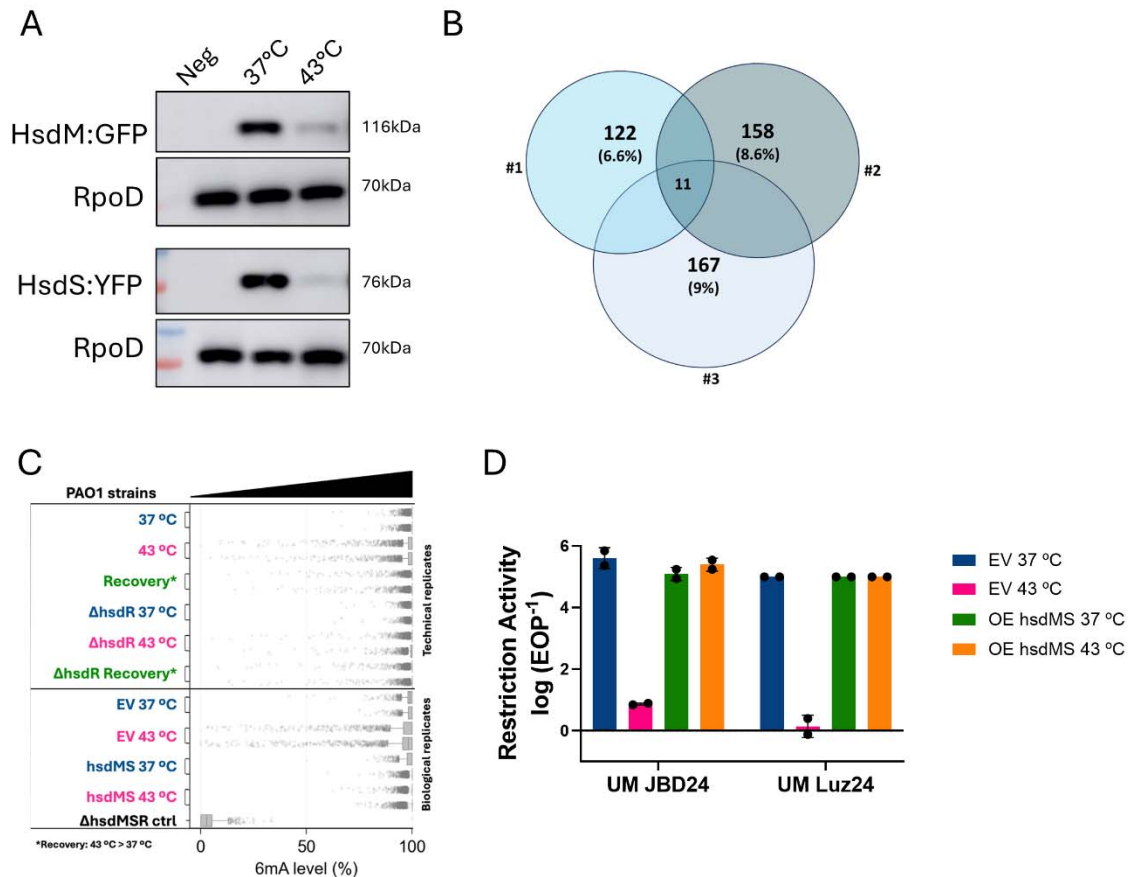
Figure 3: The IREN phenotype arises due to hypomodification during elevated temperature growth conditions. (A) Stability of modification proteins under different conditions: Western blot analysis of GFP/YFP-fusion native proteins following growth at different conditions. The presented blot is representative of one of three independent biological replicates, with RpoD as a loading ctrl. **(B-C)** Methylome analysis post-HS: (B) SMRT-seq results for WT strain grown at 43 °C compared to 37 °C. The numbers indicate the count of unmodified sites. Each circle represents one of three independent biological replicates, with shared groups representing conserved sites. (C) e-TAM analysis under different conditions: strains grown at 37 °C, 43 °C, and after initial recovery from 43 °C, single dots represent a possible modification site. Technical and biological replicates illustrate the methylation status. **(D)** OE of HsdMS at 43 °C inhibits iREN: Restriction activity of strains with empty vector and HsdMS OE initially grown at 37 °C (blue and green) or 43 °C (pink and orange), with induction at initial growth followed by sub-culturing without induction at 37 °C. Activity was measured following 10 generations at 37 °C. For (E) graphs, each dot represents an independent biological replicate.

754
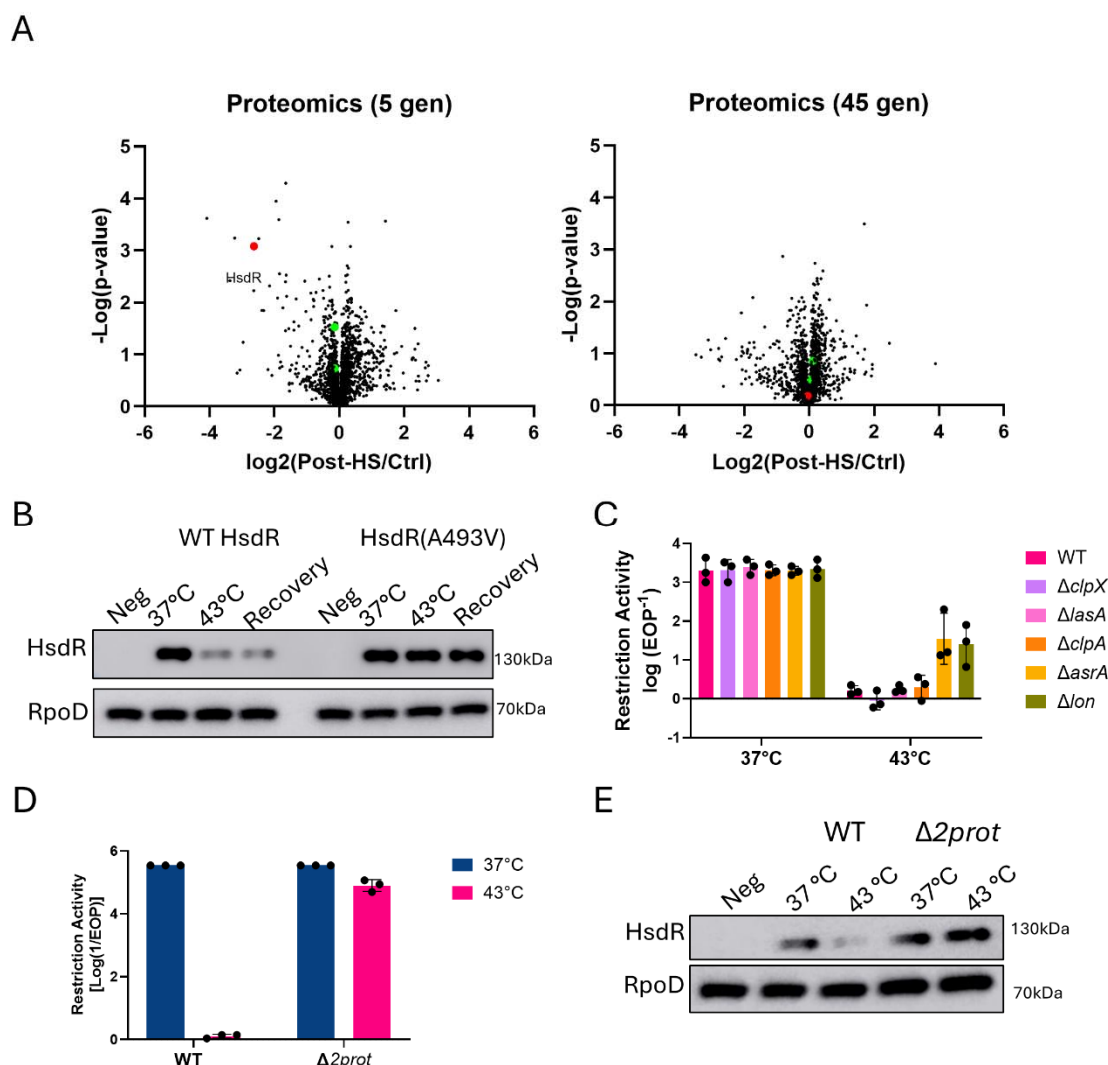
Figure 4: The restriction endonuclease levels decrease in a Lon-like protease-dependent manner. (A) Global proteomics analysis: Samples taken five generations following 43 °C growth and at the end of the recovery phase (45 generations) were compared to normal growth conditions. Marked dots indicate Hsd proteins: HsdR (red) and HsdMS (green). **(B)** Decay of HsdR protein levels with translocation activity dependence: Western blots of natively expressed HsdR:flag in WT or translocation-deficient mutant (HsdR(A493V)) strains grown at 37°C, 43°C, or sub-cultured to 37°C following ON growth at 43 °C for 5 generations. **(C)** Proteases effect on iREN: Panel of protease mutants: *clpX* (purple), *lasA* (light-pink), *clpA* (orange), *asrA* (yellow), and *lon* (green). Mutant restriction activity was measured at the end of ON growth at 37°C (left) or 43°C (right). **(D-E)** Regulation of iREN by Lon-like proteases: (D) Restriction activity following ON growth at 37 °C or 43 °C of the double proteases mutant strain compared to WT. (E) HsdR:flag native protein levels at 37°C and post-HS Δ*2prot* compared to WT. For graphs (C) and (D), each dot represents a single biological replicate, with error bars indicating standard deviation. RpoD was used as loading ctrl.

769
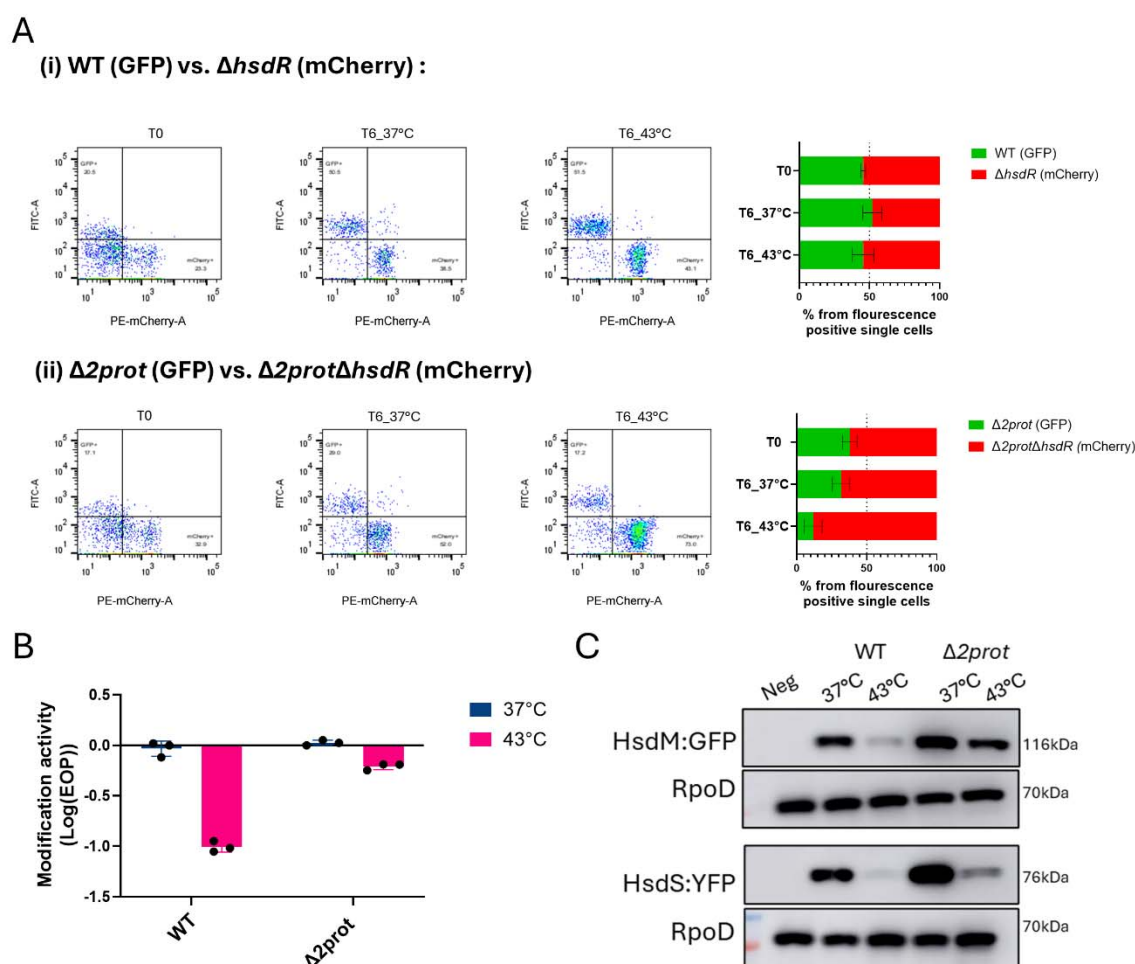
Figure 5: Proteases mutants that cannot degrade HsdR are outcompeted. (A) *hsdR* deletion competition under different conditions: Flow-cytometry analysis of population variation in mixed WT and Δ*hsdR* strains (top), or double-proteases mutant and double mutant lacking *hsdR* (bottom). Mixtures were grown for six hours before analysis. Analysis histograms are displayed for representative replicates in both conditions (left), and population percentages are shown as an average of three biological replicates (right). **(B)** Modification activity in protease mutants: Phage modification activity assay for WT and double-protease mutant Δ*2prot* at 37 °C and 43 °C. Each dot represents a single biological replicate. **(C)** Modification proteins stability in protease mutants: Western blot analysis of GFP/YFP-fusion native proteins following growth at different conditions in Δ*2prot* strain compared to WT. The presented blot is representative of one of three independent biological replicates. RpoD was used as loading ctrl.

781
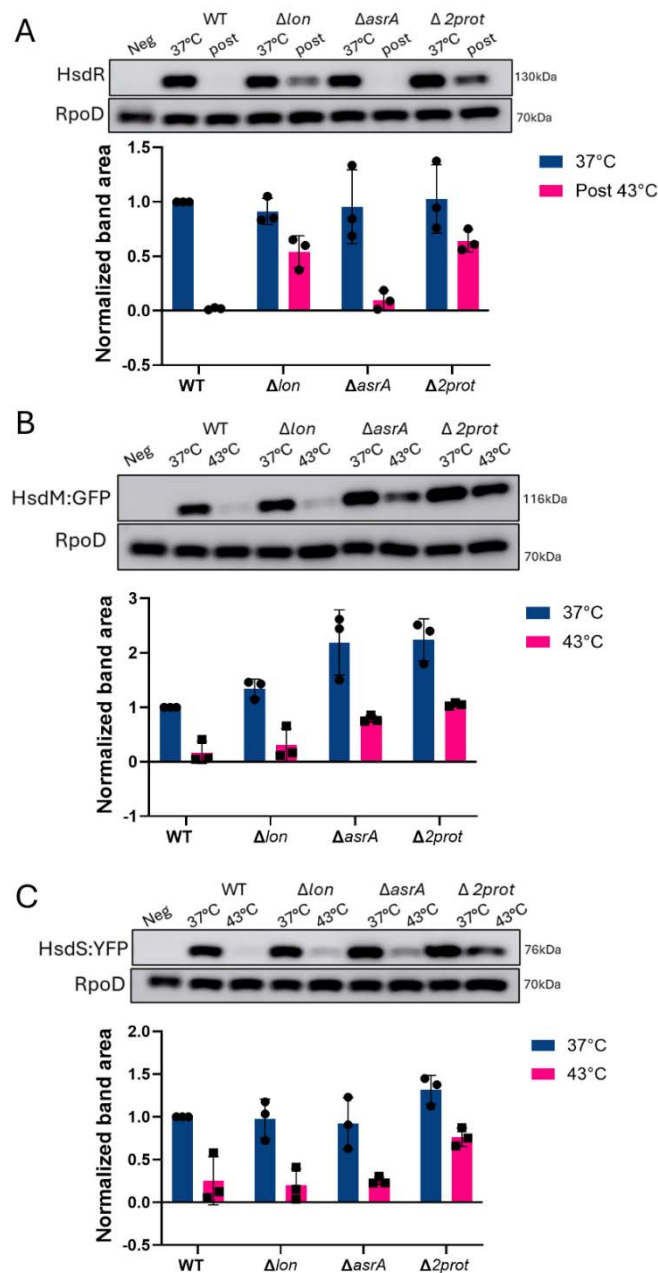
Figure 6: Lon-like proteases operate in iREN in collaborative manner. **(A)** HsdR protein levels in protease mutants: Western blot analysis of flag-fusion native HsdR protein following growth under different conditions of WT and protease mutants. The quantification of band area is normalized to the loading control (RpoD) and WT at 37 °C as a standard (bottom panel). **(B-C)** Stability of modification proteins in protease mutants: Western blot analysis of GFP/YFP-fusion native HsdM (B) and HsdS (C) proteins following initial growth under different conditions, with quantification of band area normalized to the loading control (RpoD) and WT at 37 °C as a standard (bottom panels). The blot presented is representative of one of three independent biological replicates.

791
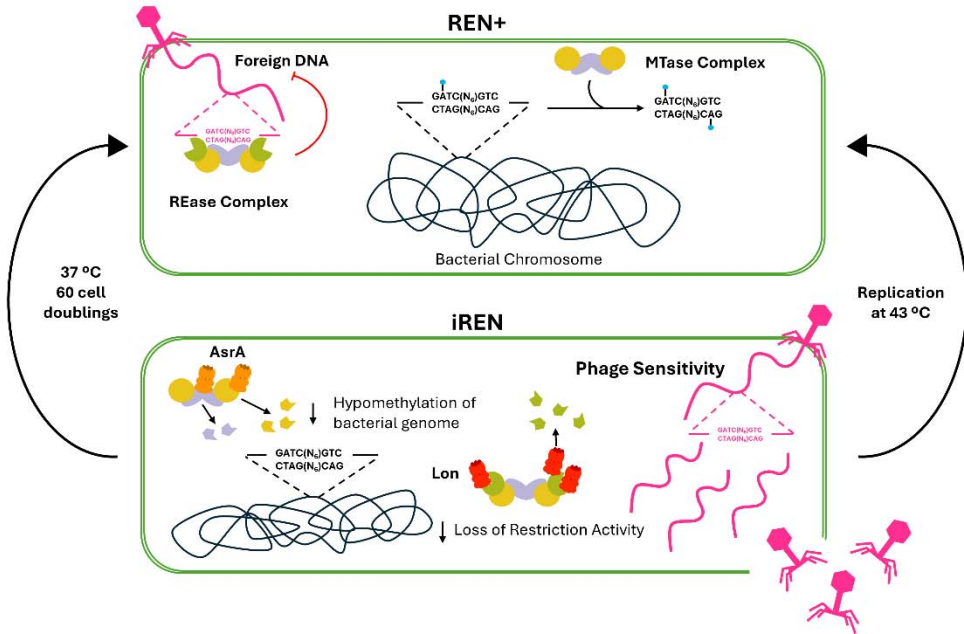
Figure 7: Proposed model for iREN. Under normal conditions (top, **R**estriction **EN**donuclease **+** or **REN+**), PAO1 maintains a functional type I R-M system, with the MTase complex (HsdM in yellow, HsdS in grey) modifying the host genome and the REase complex (including HsdR in green) restricting foreign DNA. After growth at 43 °C (bottom, **iREN**), the restriction targets unmodified sites on the bacterial chromosome, which is inhibited by Lon-like proteases (red triangle). Following approximately 60 generations of recovery at 37 °C, bacteria restore their native restriction activity.

799
800

801
802
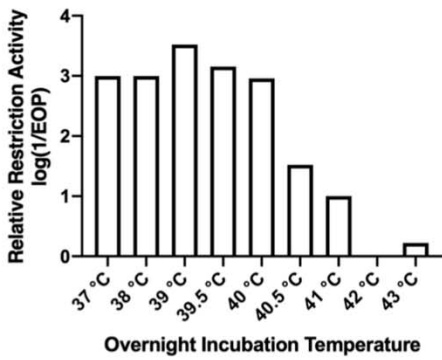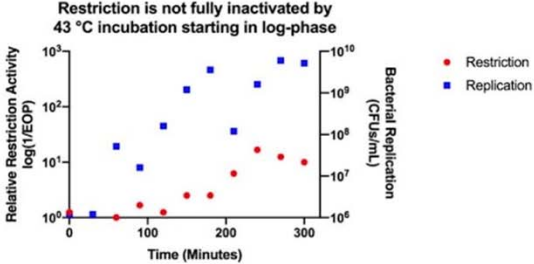
Figure S1: Dynamics and conservancy of iREN. (A) Examination of restriction activity following overnight growth at temperatures **(B)** Restriction activity (red) examined for PAO1 WT strain when incubated at 43 °C during different growth stages (blue, OD 600nm).
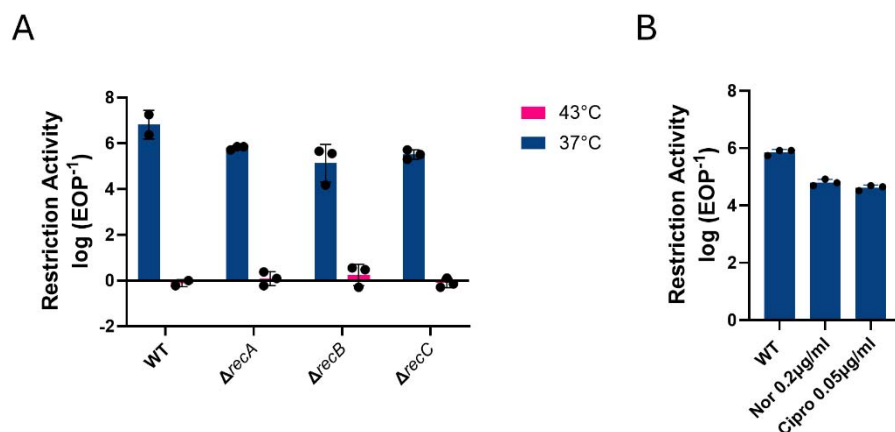
806
807 **Fig. S2: DNA recombination and breaks do not induce iREN. (A)** restriction activity
808 recombination genes mutant strains at 37 °C (blue) and following 43 °C growth, compared to WT
809 strain. **(B)** Restriction activity following 6 hr growth with sub-inhibitory concentration
810 Fluoroquinolone treatment of Ciprofloxacin and Norfloxacin, compared to untreated WT strain.
811
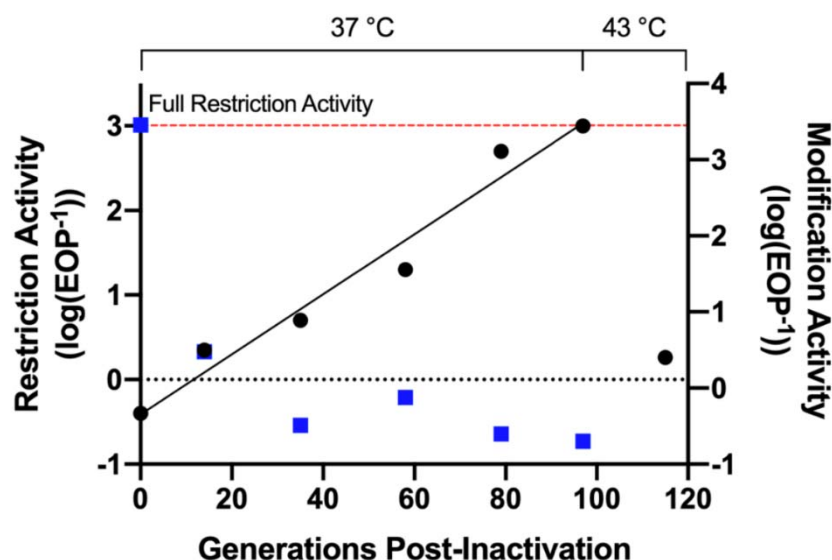
812
813
814 **Fig. S3:** Restriction activity following ON growth at 43 °C, 100 generations recovery at 37 °C, and
815 re-introducing ON growth at 43 °C.

A

**B**   **C**
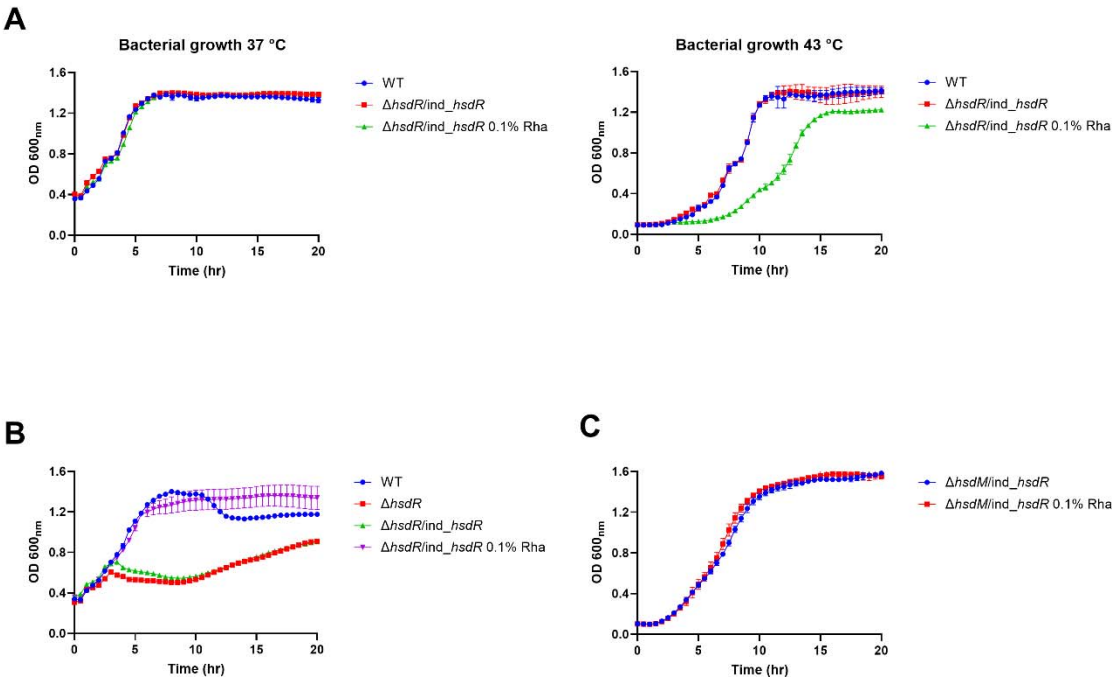
816

817   **Figure S4: HsdR expression is toxic only at iREN state.** **(A)** Growth curve at 37°C following
818   or ON growth at 37 °C (left) or 43°C (right) of WT and strains harboring an inducible copy of
819   *hsdR*, treated with Rha inducer. **(B)** Restriction activity of WT, *hsdR* mutant, and strains harboring
820   an inducible copy of *hsdR* at 37 °C, treated with Rha inducer **(C)** Growth curve at 37°C following
821   ON growth at 43°C (right) of *hsdM* mutant strain harboring an inducible copy of *hsdR* with or
822   without Rha inducer addition. For all the graphs above, inducer was added at t=0.

823   **Table S1: iREN examination in different *P. aeruginosa* strains following growth at 43 °C
824   with indicated genomic type I R-M systems**.

Pae strains*	iREN	Total Type I R-M
A5	✔	1
A6	X	0
A7	✔	2
A8	✔	2
A9	✔	2
B1	X	1
B2	X	1
B7	✔	1
B8	✔	2
B9	✔	2
B10	✔	1
C6	✔	2
PAK	✔	1
PA14	X	0
*Representative of biological replicates		

✔: Phage titers increase in strain grown at 43 ºC
X: Not detected in these conditions

825

826
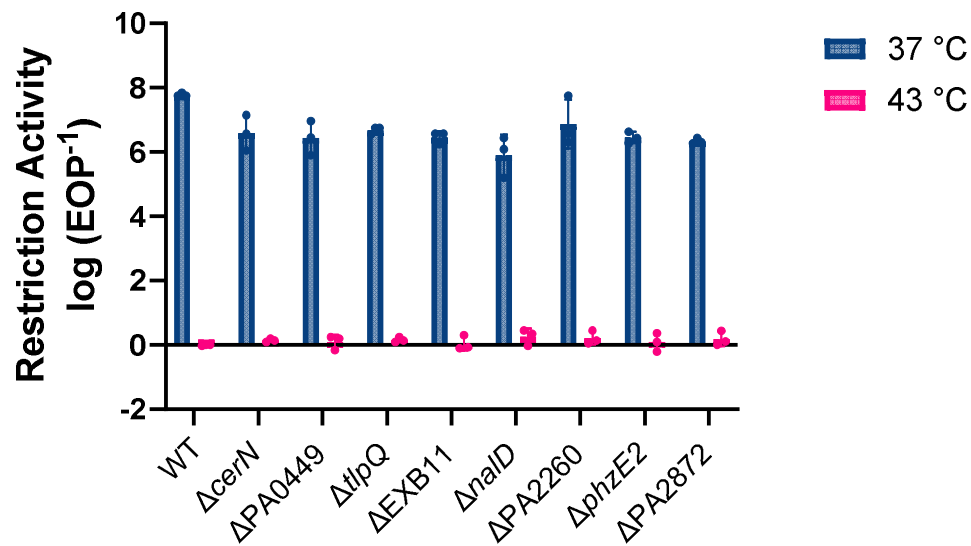
Figure S5: Modification hot spots at 43 °C do not specifically affect iREN. Restriction activity
following ON growth at 37 °C (blue) or 43 °C (pink) of WT strain and mutants. Mutants are strains
lucking the complete ORF containing the modification site. The graph is the average of three
independent biological replicates, with error bars indicating standard deviation.
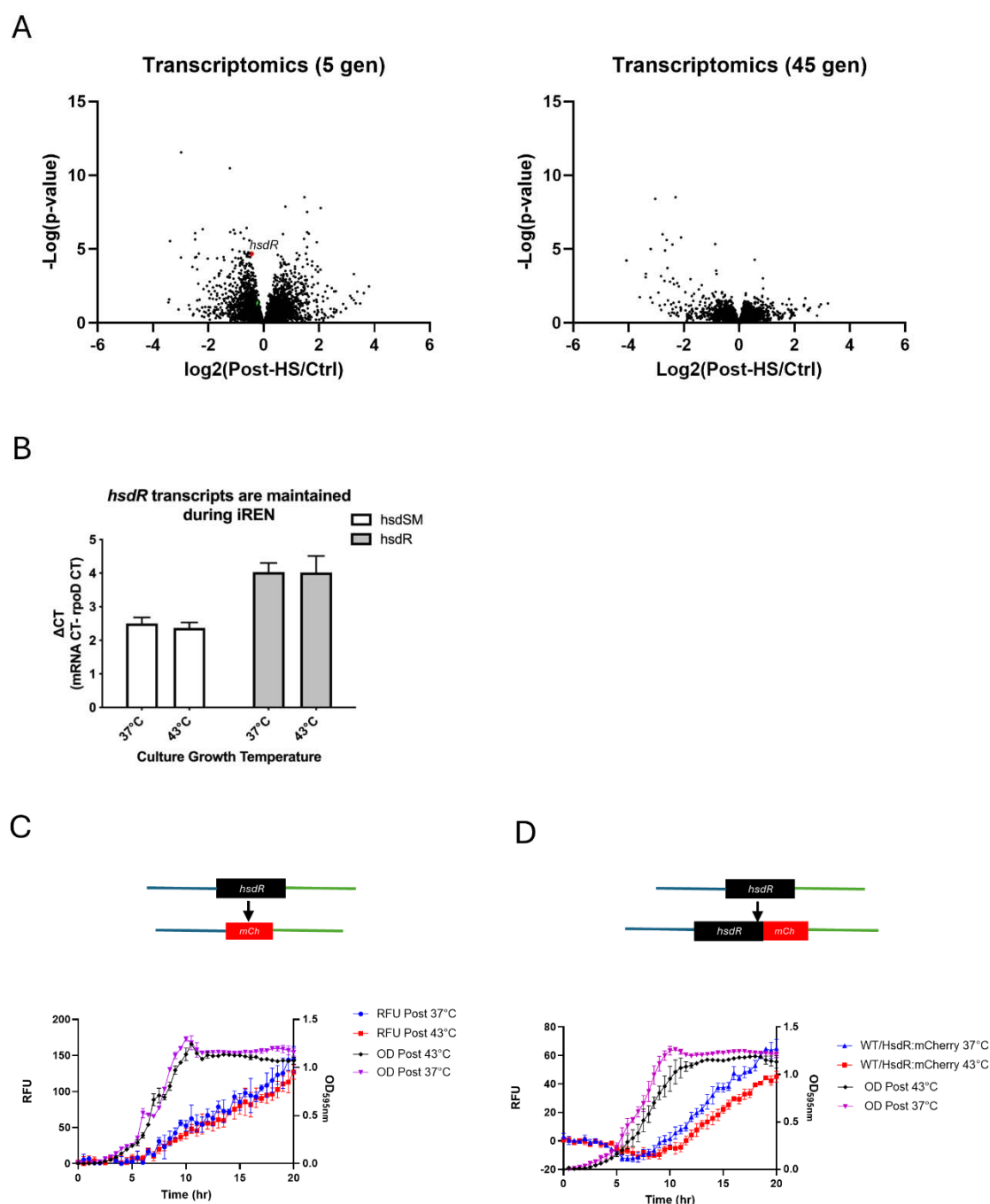
Figure S6: Restriction endonuclease is not transcriptionally regulated. (A) Global transcriptomics analysis: Samples taken 5 generations following 43 °C growth and at the end of the recovery phase (45 generations) were compared to normal growth conditions. Marked dots indicate Hsd proteins: HsdR (red) and HsdMS (green). Transcriptional and Translational Reporter Analysis. **(B)** Real-time PCR analysis of *hsd* transcripts following growth at either 37 °C or 43 °C. expression levels are normalized to *rpoD* as a ctrl. **(C)** Fluorescence and absorbance measurements over time of a strain harboring the *hsdR* ORF replaced by *mCherry*, representing transcriptional reporter analysis. **(D)** Fluorescence and optical density measurements over time of a strain harboring *hsdR* fused to *mCherry*, representing translational reporter analysis. The (C)

841 and (D) graphs are the average of three independent biological replicates, with error bars
842 indicating standard deviation.
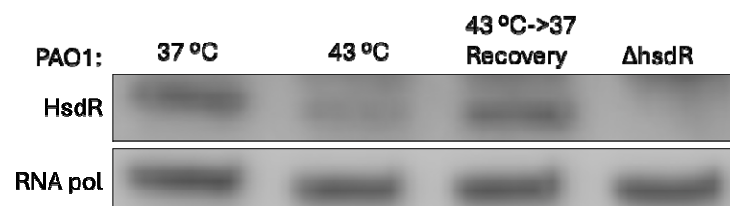
843

844 **Figure S7: HsdR-specific custom antibody which showed a similar reduction in HsdR**
845 **levels.** Endogenous measurement of Type I R-M proteins, HsdR from WT cells at 37 ºC, 43 ºC,
846 or recovery at 37 ºC for 10 generations by Western blot analysis using custom polyclonal
847 antibodies, RNA pol was used as a loading ctrl.
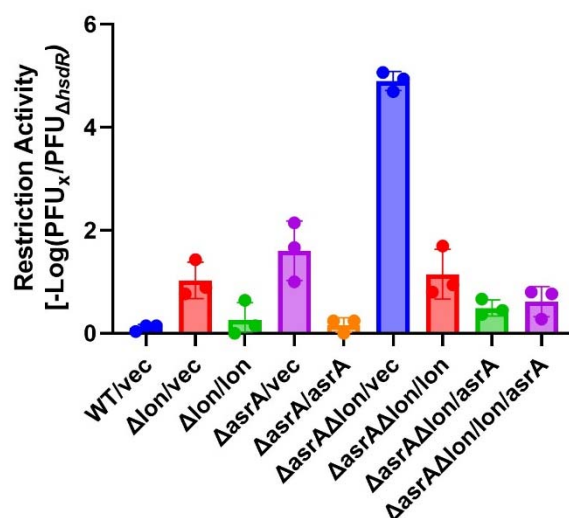
848
849 **Figure S8: Proteases complementation and HsdR protein levels effect.** Protease
850 complementation restores iREN: WT and mutant strains containing either empty vectors or
851 plasmid-expressed protease were examined for restriction activity following ON growth at 43 °C.
852 each dot represents a single biological replicate, with error bars indicating standard deviation.

(i) WT (GFP) vs. ΔhsdR (mCherry) :
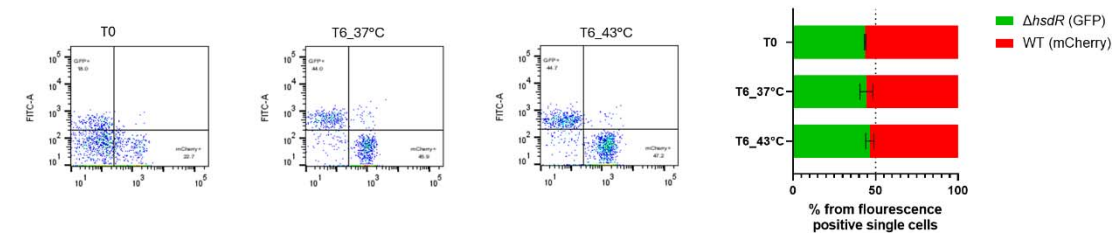
(ii) Δ2prot (GFP) vs. Δ2protΔhsdR (mCherry)
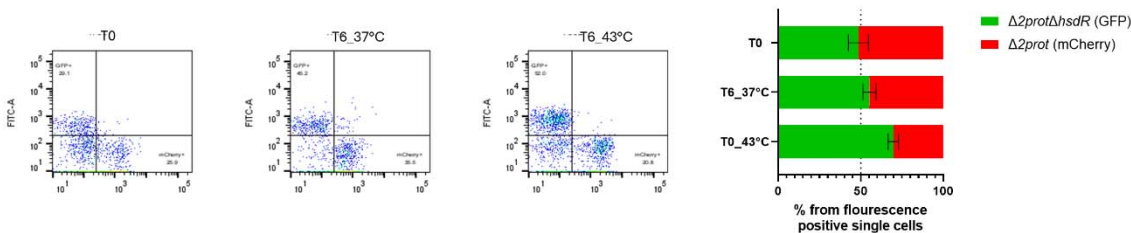
853

854 **Figure S9: Growth rate and fitness cost for restriction activation in the proteases mutant**
855 **(A)** Growth curves of WT, single mutants, and double 2prot mutants (blue) with additional deletion
856 of *hsdR* (red) at 43°C (up) and following sub-culture to 37°C (bottom). Graphs represent the
857 average of three biological replicates, with error bars indicating standard deviation. **(B)** *hsdR*
858 deletion competition under different conditions, reverse tagging: Flow-cytometry analysis of
859 population variation in mixed WT and ∆*hsdR* strains (top), or double-proteases mutant and
860 double mutant lacking *hsdR* (bottom). Mixtures were grown for six hours before analysis.
861 Representative histograms of the reverse tagging analysis are displayed (left), and population
862 percentages are shown as an average of three biological replicates (right).

863 **Table S2:** Strains and plasmids used in the study

Strain or plasmid	Description	Source
P. aeruginosa strains		
PA01	Wild-type *P. aeruginosa*	32
PA14	burn wound isolate of *P. aeruginosa*	18
PAK	PAK (PA06) human cystic fibrosis isolate of *P. aeruginosa*	18
A5	PA100420 human cystic fibrosis isolate of *P. aeruginosa*	18
A6	PA1032 human acute infection-respiratory tract isolate of *P. aeruginosa*	18
A7	CF040 human cystic fibrosis isolate of *P. aeruginosa*	18
A8	EnvJH soil isolate of *P. aeruginosa*	18
A9	RYC25616 human cystic fibrosis isolate of *P. aeruginosa*	18
A12	CFS2 human cystic fibrosis isolate of *P. aeruginosa*	18
B1	114199 human sputum isolate of *P. aeruginosa*	18
B2	RR1 oil-contaminated soil isolate of *P.*	18

	aeruginosa	
B7	PA191517 human cystic fibrosis isolate of *P. aeruginosa*	18
vB8	PA87110594 human endotracheal tube isolate of *P. aeruginosa*	18
B9	PA4944 human rectal swab isolate of *P. aeruginosa*	18
B10	PA100683 human cornea isolate of *P. aeruginosa*	18
C8	PA2046 human acute infection-respiratory tract	18
PAO1_JBD24	PAO1 lysogen of JBD24	This study
Δ*hsdR*	PAO1 with PA2732 gene deletion	13
Δ*hsdMSR*	PAO1 with PA2732-5 genes deletion	This study
Δ*hsdM*	PAO1 with PA2735 genes deletion	This study
hsdR transcriptional reporter	PAO1 with mCherry replacing PA2732 ORF	This study
hsdR translational reporter	PAO1 with mCherry fused to C' PA2732 ORF	This study
hsdR:FLAG	PAO1 with FLAG tag fused to N' PA2732 ORF	This study
hsdR(A493V)	PAO1 with A493V substitution in PA2732 ORF	This study
hsdR(A493V):FLAG	PAO1 with FLAG tag fused to N' PA2732 ORF with A493V substitution	This study
HsdR OE	PAO1 with pJN105_hsdR	This study
Δ*hsdR*/*hsdR*	Δ*hsdR* with genomic pUCP18T-miniTN7T-Gm_pRha_hsdR	This study
Δ*hsdM*/*hsdR*	Δ*hsdM* with genomic pUCP18T-miniTN7T-Gm_pRha_hsdR	This study
hsdM:GFP	PAO1 with GFP fused to C' PA2735 ORF	This study
hsdS:YFP	PAO1 with YFP fused to C' PA2734 ORF	This study
PAO1 EV	PAO1 with empty pHERT30	This study
PAO1 hsdMS	PAO1 with hsdMS on pHERT30	This study
Δ*clpX*	PAO1 with *clpX* gene deletion	This study
Δ*lasA*	PAO1 with *lasA* gene deletion	This study
Δ*clpA*	PAO1 with *clpA* gene deletion	This study
Δ*asrA*	PAO1 with *asrA* gene deletion	This study
Δ*lon*	PAO1 with *lon* gene deletion	This study
Δ*2prot*	PAO1 with *lon* and *asrA* gene deletion	This study
Δ*2prot*/*hsdR*:FLAG	Δ*2prot* with FLAG tag fused to N' PA2732 ORF	This study
Δ*lon*/*hsdR*:FLAG	Δ*lon* with FLAG tag fused to N' PA2732 ORF	This study
Δ*asrA*/*hsdR*:FLAG	Δ*asrA* with FLAG tag fused to N' PA2732 ORF	This study
Δ*2prot*/*hsdM*:GFP	Δ*2prot* with GFP fused to C' PA2735 ORF	This study
Δ*lon*/*hsdM*:GFP	Δ*lon* with GFP fused to C' PA2735 ORF	This study
Δ*asrA*/*hsdM*:GFP	Δ*asrA* with GFP fused to C' PA2735 ORF	This study
Δ*2prot*/*hsdS*:YFP	Δ*2prot* with YFP fused to C' PA2734 ORF	This study
Δ*lon*/*hsdS*:YFP	Δ*lon* with YFP fused to C' PA2734 ORF	This study
Δ*asrA*/*hsdS*: YFP	Δ*asrA* with YFP fused to C' PA2734 ORF	This study
Δ*2prot*Δ*hsdR*	PAO1 with *lon*, *asrA,* and PA2732 genes deletion	This study
Δ*2prot*_JBD24	Δ*2prot* lysogen of JBD24	This study
PAO1_GFP	PAO1 with pUCP18-Ap_GFP	This study
PAO1_mCherry	PAO1 with pUCP18-Ap_mCherry	This study
Δ*2prot*_GFP	Δ*2prot* with pUCP18-Ap_GFP	This study
Δ*2prot*_mCherry	Δ*2prot* with pUCP18-Ap_mCherry	This study
Δ*hsdR*_GFP	Δ*hsdR* with pUCP18-Ap_GFP	This study
Δ*hsdR*_mCherry	Δ*hsdR* with pUCP18-Ap_mCherry	This study
Δ*2prot*Δ*hsdR*_GFP	Δ*2prot*Δ*hsdR* with pUCP18-Ap_GFP	This study
Δ*2prot*Δ*hsdR*_mCherry	Δ*2prot*Δ*hsdR* with pUCP18-Ap_mCherry	This study
Δ*recA*	PAO1 with *recA* gene deletion	This study
Δ*recB*	PAO1 with *recB* gene deletion	This study
Δ*recC*	PAO1 with *recC* gene deletion	This study
Δ*cerN*	PAO1 with *cerN* gene deletion	This study
Δ*PA0449*	PAO1 with PA0449 gene deletion	This study
Δ*tlpQ*	PAO1 with *tlpQ* gene deletion	This study

ΔEXB11	PAO1 with EXB11 gene deletion	This study
Δ*nalD*	PAO1 with *nalD* gene deletion	This study
ΔPA2260	PAO1 with PA2260 gene deletion	This study
Δ*phzE2*	PAO1 with *phzE2* gene deletion	This study
ΔPA2872	PAO1 with PA2872 gene deletion	This study
WT/vec	PAO1 with empty pJN105 and pUCP18-Ap vectors	This study
Δ*lon*/vec	Δ*lon* with empty pJN105 and pUCP18-Ap vectors	This study
Δ*asrA*/vec	Δ*asrA* with empty pJN105 and pUCP18-Ap vectors	This study
Δ*2prot*/vec	Δ*2prot* with empty pJN105 and pUCP18-Ap vectors	This study
Δ*lon*/lon	Δ*lon* with pJN105_lon and empty pUCP18-Ap vectors	This study
Δ*asrA*/asrA	Δ*asrA* with empty pJN105 and pUCP18-Ap_asrA vectors	This study
Δ*2prot*/lon	Δ*2prot* with pJN105_lon and empty pUCP18-Ap vectors	This study
Δ*2prot*/asrA	Δ*2prot* with empty pJN105 and pUCP18-Ap_asrA vectors	This study
Δ*2prot*/lon/asrA	Δ*2prot* with pJN105_lon and pUCP18-Ap_asrA vectors	This study
***E. coli* strains**		
DH5α	F⁻ Φ80lacZΔM15 Δ(lacZYA-argF) U169 recA1 endA1 hsdR17 (rK-, mK+) phoA supE44 λ- thi-1 gyrA96 relA1.	Bio-Lab
S17	*E. coli* S17 thi, pro, hsdR, recA::RP4 -2-Tc::Mu aphA::Tn7, λ-pir, Smr , Tpr	[33]
Plasmids		
pUCP18-Ap	Crbʳ (for *P. aeruginosa*), Ampʳ (for *E. coli*), overexpression plasmid, *lacZ* promoter	[34]
pDONRPEX18Gm	Gmʳ and Cmʳ, pEX18Gm containing a HindIII flanked, *attP* cloning site from pDONR201	[35]
pUCP18T-miniTN7T-Gm	Ampʳ and Gmʳ; Gmr on mini-Tn7T, mobilizable suicide plasmid	[36]
pJN105	Overexpression plasmid under araC promoter	[37]
pHERT30	Gmʳ, overexpression plasmid under araC promoter	[38]
pDONRPEX18Gm_asrA_ko	For clean *asrA* gene deletion	This study
pDONRPEX18Gm_cerN_ko	For clean *cerN* gene deletion	This study
pDONRPEX18Gm_clpA_ko	For clean *clpA* gene deletion	This study
pDONRPEX18Gm_clpX_ko	For clean *clpX* gene deletion	This study
pDONRPEX18Gm_EXB11_ko	For clean EXB11 gene deletion	This study
pDONRPEX18Gm_hsdM_GFP	For fusion GFP to C' PA2735	This study
pDONRPEX18Gm_hsdM_ko	For clean PA2735 gene deletion	This study
pDONRPEX18Gm_hsdR_A493V	For A493V substitution in PA2732 gene	This study
pDONRPEX18Gm_hsdR_A493V_Flag	For fusion FLAG tag to N' PA2732 with A493V substitution	This study
pDONRPEX18Gm_hsdR_flag	For fusion FLAG tag to N' PA2732	This study
pDONRPEX18Gm_hsdR_mCherry	For fusion mCherry to C' PA2732	This study
pDONRPEX18Gm_hsdS_YFP	For fusion YFP to C' PA2734	This study
pDONRPEX18Gm_lasA_ko	For clean *lasA* gene deletion	This study
pDONRPEX18Gm_lon_ko	For clean *lonA* gene deletion	This study
pDONRPEX18Gm_nalD_ko	For clean *nalD* gene deletion	This study
pDONRPEX18Gm_PA0449_ko	For clean PA0449 gene deletion	This study

pDONRPEX18Gm_PA2260_ko	For clean PA2260 gene deletion	This study
pDONRPEX18Gm_PA2872_ko	For clean PA2872 gene deletion	This study
pDONRPEX18Gm_phsdR_mCherry	For replacing PA2732 gene with mCherry	This study
pDONRPEX18Gm_phzE2_ko	For clean *phzE2* gene deletion	This study
pDONRPEX18Gm_recA_ko	For clean *recA* gene deletion	This study
pDONRPEX18Gm_recB_ko	For clean *recB* gene deletion	This study
pDONRPEX18Gm_recC_ko	For clean *recC* gene deletion	This study
pDONRPEX18Gm_tlpQ_ko	For clean *tlpQ* gene deletion	This study
pHERT30_hsdMS	For hsdMS expression	This study
pJN105_hsdR	For PA2732 expression	This study
pJN105_lon	For *lon* expression	This study
pUCP18-Ap_asrA	For *asrA* expression	This study
pUCP18-Ap_GFP	For GFP expression	This study
pUCP18-Ap_mCherry	For mCherry expression	This study
pUCP18T-miniTN7T-Gm_pRha_hsdR	For PA2732 expression under Rhamnose promoter	This study
	Phages	
JBD24	Temperate phage of *P. aeruginosa*	[18]
JBD30	Temperate phage of *P. aeruginosa*	[18]
Luz24	Lytic phage of *P. aeruginosa*	[39]

864